

Finite temperature fermionic charge and current densities in conical space with a circular edge

A. A. Saharian*, V. F. Manukyan†, T. A. Petrosyan‡

*Institute of Physics, Yerevan State University,
1 Alex Manoogian Street, 0025 Yerevan, Armenia*

April 22, 2025

Abstract

We study the finite temperature and edge induced effects on the charge and current densities for a massive spinor field localized on a 2D conical space threaded by a magnetic flux. The field operator is constrained on a circular boundary, concentric with the cone apex, by the bag boundary condition and by the condition with the opposite sign in front of the term containing the normal to the edge. In two-dimensional spaces there exist two inequivalent representations of the Clifford algebra and the analysis is presented for both the fields realizing those representations. The circular boundary divides the conical space into two parts, referred as interior (I-) and exterior (E-) regions. The radial current density vanishes. The edge induced contributions in the expectation values of the charge and azimuthal current densities are explicitly separated in the both regions for the general case of the chemical potential. They are periodic functions of the magnetic flux and odd functions under the simultaneous change of the signs of magnetic flux and chemical potential. An important difference from the fermion condensate, considered previously in the literature, is that the mean charge and current densities are finite in the limit when the observation point tends to the boundary. In the E-region all the spinorial modes are regular and the total charge and current densities are continuous functions of the magnetic flux. In the I-region the corresponding expectation values are discontinuous at half-integer values of the ratio of the magnetic flux to the flux quantum. Those discontinuities come from the contribution of the irregular mode in the I-region. 2D fermionic models, symmetric under the parity and time-reversal transformations (in the absence of magnetic fields) combine two spinor fields realizing the inequivalent representations of the Clifford algebra. The total charge and current densities in those models are discussed for different combinations of the boundary conditions for separate fields. Applications are discussed for electronic subsystem in graphitic cones described by the 2D Dirac model.

Keywords: Fermionic charge and current, conical space, Casimir effect, persistent currents

1 Introduction

The investigation of (2+1)-dimensional field-theoretical models is motivated by several reasons. Despite the low dimensionality, these models may exhibit a rich variety of properties that can reveal insights into theories with higher dimensionality, providing a testing ground for effects which are more complicated

*E-mail: saharian@ysu.am

†E-mail: vardan.manukyan@ysu.am

‡E-mail: tigran.petrosyan@ysu.am

for the analysis in 4-dimensional spacetime. The 2D models often allow for exact solutions and detailed analytical studies that are not feasible in higher dimensions. These models appear as high temperature limits of (3+1)-dimensional field theories and describe the low energy dynamics of excitations in condensed matter systems [1, 2]. An interesting area of research is the lower dimensional gravity [3] which provides unique tools for studying gravitational interactions with reduced complexity. The corresponding models can shed light on the nature of spacetime, black holes, and quantum gravity, potentially extending our understanding of higher-dimensional theories of gravity. The 2D theories foster interdisciplinary research between high-energy physics, condensed matter physics, and mathematical physics. These models involve rich mathematical structures, such as modular forms and braid groups. Many physical phenomena in Dirac materials such as graphene, topological insulators and Weyl semimetals can be effectively explained by 2D theories. For those systems, the long-wavelength excitations of electronic subsystem are described by the Dirac equation with the velocity of light replaced by the Fermi velocity which is nearly 300 times smaller [4]-[6]. As a result, an opportunity is opened for the investigation of the relativistic effects at lower velocities. Moreover, the Coulomb interaction is strongly renormalized on the graphite sheet. In 3D topological insulators, the two dimensional massless fermionic excitations appear as edge states on the surface. The quantum Hall effect and other topological phases of matter, observed in condensed matter physics, exhibit exotic properties such as fractional statistics and topologically protected edge states, which can be effectively described using (2+1)-dimensional field theories. In (2+1) dimensions, gauge theories with Chern-Simons terms are of particular interest. These terms lead to novel features like topological mass generation and have applications in both high-energy physics and condensed matter systems, such as anyonic excitations in fractional quantum Hall systems [7].

In a number of 2D models of quantum field theory, including those describing condensed matter systems, the physical degrees of freedom are confined to finite regions by imposing different types of periodicity and boundary conditions. Additional conditions on the fields are also imposed in problems with different sorts of topological defects. Understanding how the boundary conditions affect the behavior of quantum fields in (2+1) dimensions can lead to more realistic and applicable models. Investigating the edge-induced effects in (2+1) spacetime dimensions can also provide insights into the AdS/CFT correspondence, where the (2+1)-dimensional quantum theory is considered on the boundary of a (3+1)-dimensional AdS spacetime. The latter can enhance our understanding of the importance of holography related to the string theory and quantum gravity. In the context of field theories the boundary conditions modify the spectrum of quantum fluctuations, thereby giving rise to boundary-induced contributions in the expectation values of physical characteristics. This type of shift is known as the Casimir effect, which has been the subject of extensive research due to its significance in diverse areas of fundamental physics and micromechanical applications. Investigations have been conducted for a broad spectrum of boundary and background geometries (for reviews see [8]-[11]). A series of analogous effects emerge in models with compact spatial dimensions as a consequence of the compactification conditions imposed on the fields (topological Casimir effect).

Another field of active research is the investigation of the effects caused by a finite temperature on 2D systems, impacting their physical properties and behavior. Considering these temperature-dependent effects is critical for the practical application of 2D materials in various technologies, including optoelectronics, sensors, and nanotechnology. Finite temperature induces thermal fluctuations that can affect the structural integrity by causing sometimes to the formation of ripples or other deformations in the material. Additionally, the electronic, magnetic and optical properties can be significantly influenced by finite temperature. By increasing the thermal energy it is possible to affect the mobility of charge carriers, conductivity, and band structure. For example, in semiconducting 2D materials, temperature can impact the band gap and carrier concentration. For instance, the effects of the Coulomb interaction in multi-walled carbon nanotubes have been observed by several electrical transport experiments. At temperatures lower than 1 K, the Coulomb blockade regime appears where the tunneling transparency of a barrier vanishes in the device due to the interactions between electrons. When the temperature increases, the Luttinger liquid regime may be formed. The transition from one regime to another is theo-

retically studied in [12]. At very high temperatures, the thermal agitation can disrupt magnetic ordering in 2D materials, potentially leading to a transition from ferromagnetic to paramagnetic states. Changes in temperature can alter the absorption and emission properties, the band structure and exciton binding energy, as a result, changing the way how the material interacts with light.

In the present paper we investigate the combined effects of nontrivial topology and boundary on the finite temperature fermionic charge and current densities for a massive field in (2+1)-dimensional conical spacetime. The latter appears as an effective geometry in field-theoretical models describing 2D condensed matter systems and as a subspace of the geometry outside straight cosmic strings. The formation of topological defects of cosmic string type during phase transitions in the early universe may have significant implications for astrophysics and cosmology [13, 14]. An illustrative example of condensed matter systems exhibiting effective conical geometry is that of graphitic cones [15]-[25]. The effects of nontrivial topology of a conical space on the local characteristics of the vacuum state for quantum fields have been extensively examined in the existing literature (see, e.g., the references in [26]). In this study, the expectation values of the field squared, fermion condensate and energy-momentum tensor were considered as key characteristics. In conical geometries with magnetic fluxes within the core, another noteworthy phenomenon is the emergence of azimuthal vacuum currents [27]-[36] (the vacuum currents in more general curved 2D geometries were studied in [37]). The boundary-induced Casimir effect for the current density in conical geometries has been investigated in [26, 31]. The influence of the defect core of finite thickness on the vacuum current was discussed in [38]. The current density in conical spacetimes with local de Sitter and anti-de Sitter geometries were studied in [39]-[43] (for vacuum currents in de Sitter and anti-de Sitter spacetimes with a part of dimensions compactified on a torus see [44] and references therein).

The organization of the paper is as follows. In the next section we describe the field, the boundary condition and the background geometry. The complete set of mode functions is given for the regions outside and inside a circular boundary. In Section 3 we summarize the results for the vacuum expectation values in a conical space with a circular boundary and for the finite temperature charge and current densities in a boundary-free conical space. The finite temperature expectation values of the charge and current densities outside and inside a circular boundary in 2D conical space are evaluated in Sections 4 and 5. The boundary-induced contributions are explicitly separated in the expectation values. The asymptotic behavior of the boundary-induced parts in the limiting regions of the parameters is described and numerical analysis is presented in Section 6. The main results of the paper are summarized in Section 8. Appendix A contains some intermediate calculations which are needed for the final expressions of the expectation values in the exterior region in the cases of nonzero and zero chemical potentials. An alternative derivation of the zero temperature limits of the expectation values of the charge and current densities is presented in Appendix B.

2 Problem setup and fermionic modes

In this section we present the complete set of fermionic mode functions for a conical geometry in the presence of a circular boundary. We begin with the (3+1)-dimensional flat spacetime line element written in terms of spherical coordinates $(r, \theta, \tilde{\phi})$ with a fixed value of the polar coordinate $\theta = \theta_0$. It has the form $ds^2 = dt^2 - dr^2 - r^2 \sin^2 \theta_0 d\tilde{\phi}^2$ where r takes non-negative values and $0 \leq \tilde{\phi} < 2\pi$. Introducing a new azimuthal coordinate $\phi = \tilde{\phi} \sin \theta_0$ with the variation range $0 \leq \phi < 2\pi \sin \theta_0 \equiv \phi_0$, the expression for the line element reads

$$ds^2 = g_{\mu\nu} dx^\mu dx^\nu = dt^2 - dr^2 - r^2 d\phi^2. \quad (2.1)$$

In general, this corresponds to a conical spacetime described in terms of spatial polar coordinates (r, ϕ) . The point $r = 0$ corresponds to the apex of a cone with a planar angle deficit $2\pi - \phi_0$. In the special case $\phi_0 = 2\pi$ the bulk coincides with the (2+1)-dimensional Minkowski spacetime.

We consider a spinor field $\psi(x)$ in the presence of an external electromagnetic field with the vector potential $A_\mu = (0, 0, A)$ having a constant angular component $A_2 = A$. This means that the physical component of the vector potential is expressed as $A_\phi = -A/r$. The latter corresponds to an infinitely thin magnetic flux $\Phi = -\phi_0 A$ located at $r = 0$. The spinor field operator obeys the Dirac equation

$$(i\gamma^\mu D_\mu - sm) \psi(x) = 0. \quad (2.2)$$

Here, we use the units $\hbar = c = 1$, m is the field mass and the parameter $s = \pm 1$ describes two inequivalent irreducible representations of the Clifford algebra (see the discussion in Section 7 below). The gauge covariant derivative in the Dirac equation is defined as $D_\mu = \partial_\mu + \Gamma_\mu + ieA_\mu$, where Γ_μ is the spin connection and e is the charge of the field quantum. The spin connection has the form

$$\Gamma_\mu = \frac{1}{4} \gamma^{(a)} \gamma^{(b)} e_{(a)}^\nu e_{(b)\nu;\mu}, \quad a, b = 0, 1, 2, \quad (2.3)$$

where the flat spacetime Dirac matrices $\gamma^{(a)}$ are expressed in terms of the Pauli matrices σ_μ as

$$\gamma^{(0)} = \sigma_3, \quad \gamma^{(1)} = i\sigma_1, \quad \gamma^{(2)} = i\sigma_2. \quad (2.4)$$

A convenient form for the basis tetrads $e_{(a)}^\mu$ is given by

$$e_{(0)}^\mu = \delta_0^\mu, \quad e_{(1)}^\mu = \left(0, \cos(q\phi), -\frac{1}{r} \sin(q\phi) \right), \quad e_{(2)}^\mu = \left(0, \sin(q\phi), \frac{1}{r} \cos(q\phi) \right), \quad (2.5)$$

where we have introduced the parameter $q = 2\pi/\phi_0 \geq 1$. For the completeness of discussion we present the form of the curved spacetime Dirac matrices $\gamma^\mu = e_{(a)}^\mu \gamma^{(a)}$ as well:

$$\gamma^1 = i \begin{pmatrix} 0 & e^{-iq\phi} \\ e^{iq\phi} & 0 \end{pmatrix}, \quad \gamma^2 = \frac{1}{r} \begin{pmatrix} 0 & e^{-iq\phi} \\ -e^{iq\phi} & 0 \end{pmatrix}, \quad (2.6)$$

and $\gamma^0 = \sigma_3$.

Additionally, we assume the presence of a circular boundary located at $r = a$ which divides the space into two separate regions. The region $r \leq a$ inside the boundary will be called as an interior region (I-region). Similarly, the region $r \geq a$ outside the circle will be referred to as the exterior region (E-region). These regions with circular boundaries, embedded in three-dimensional Euclidean space with a magnetic flux, are depicted in Figure 1. We will denote the unit normal to the boundary having an inward direction

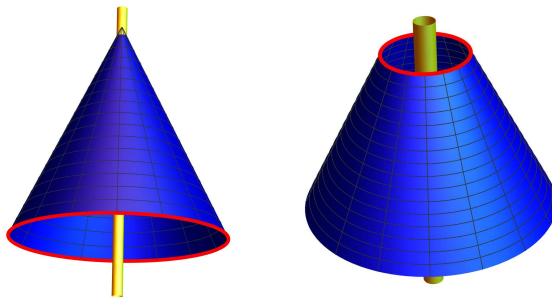


Figure 1: The I- and E-regions of a conical space with a circular edge.

by n_μ . Thus, we have $n_\mu = \delta^{(J)} \delta_\mu^1$, where $J = I$ and $J = E$ for the I- and E-regions, respectively, and

$$\delta^{(J)} = \begin{cases} 1, & J = I \\ -1, & J = E \end{cases}. \quad (2.7)$$

Further, it is assumed that at $r = a$ the field operator obeys the MIT bag boundary condition

$$(1 + in_\mu \gamma^\mu) \psi(x) = 0, \quad r = a. \quad (2.8)$$

This presents the most frequently used condition for confining fermions. The charge and current densities for the boundary condition that differs from (2.8) by the sign in front of the term involving the normal are discussed at the end of Section 5. Note that the radius of the bounding circle in the embedding 3D Euclidean space is given by $a_e = a/q$. In the part of the problem considering the expectation values in the E-region the radius a_m of the location of magnetic flux can be arbitrary in the range $a_m < a_e$.

Let $\{\psi_\sigma^{(+)}(x), \psi_\sigma^{(-)}(x)\}$ be the complete normalized set of the positive- and negative-energy mode functions obeying the equation (2.2). Here σ is the set of quantum numbers specifying the modes. The expansion of the field operator in terms of those functions has the form

$$\psi = \sum_\sigma \left[a_\sigma \psi_\sigma^{(+)} + b_\sigma^\dagger \psi_\sigma^{(-)} \right], \quad (2.9)$$

where the creation and annihilation operators obey the standard anticommutation relations.

The mode functions $\psi_\sigma^{(\pm)}(x)$ for the physical system under consideration can be found, for example, in [45] and here we present them for further references. Those functions are specified by the quantum numbers (γ, j) , with $j = \pm 1/2, \pm 3/2, \dots$, and have the form

$$\psi_\sigma^{(\pm)}(x) = c^{(\pm)} e^{iqj\phi \mp iEt} \begin{pmatrix} Z_{\beta_j}^{(\pm)}(\gamma r) e^{-iq\phi/2} \\ \epsilon_j \frac{\gamma e^{iq\phi/2}}{\pm E + sm} Z_{\beta_j + \epsilon_j}^{(\pm)}(\gamma r) \end{pmatrix}, \quad (2.10)$$

where $E = E_\sigma = \sqrt{\gamma^2 + m^2}$ stands for the energy and $Z_{\beta_j}^{(\pm)}(\gamma r)$ is a cylindrical function of the order

$$\beta_j = \alpha_j - \epsilon_j/2, \quad \alpha_j = q|j + \alpha|. \quad (2.11)$$

Here we use the notations $\epsilon_j = \text{sgn}(j + \alpha)$ and

$$\alpha = \frac{eA}{q} = -\frac{e\Phi}{2\pi}. \quad (2.12)$$

By taking into account that $\Phi_0 = 2\pi/e$ is the quantum of magnetic flux, the parameter α is interpreted in terms of the ratio of the magnetic flux and flux quantum. In the discussion below it will be shown that, the expectation values of the charge and current densities depend only on the fractional part of α . This is a characteristic feature of the Aharonov-Bohm type effects.

The radial functions in the I- and E-regions are given by the expressions

$$Z_\nu^{(\pm)}(\gamma r) = \begin{cases} J_\nu(\gamma r), & r < a \\ g_{\beta_j, \nu}^{(\pm)}(\gamma a, \gamma r), & r > a \end{cases}, \quad (2.13)$$

where we have defined the function

$$g_{\beta_j, \nu}^{(\pm)}(\gamma a, \gamma r) = \bar{Y}_{\beta_j}^{(\pm)}(\gamma a) J_\nu(\gamma r) - \bar{J}_{\beta_j}^{(\pm)}(\gamma a) Y_\nu(\gamma r). \quad (2.14)$$

Here $J_\nu(x)$ and $Y_\nu(x)$ are the Bessel and Neumann functions and the notation with the bar is defined as

$$\begin{aligned} \bar{F}_{\beta_j}^{(\pm)}(z) &= z F'_{\beta_j}(z) - \left[\epsilon_j \beta_j - \delta^{(J)}(sm_a \pm \sqrt{z^2 + m_a^2}) \right] F_{\beta_j}(z) \\ &= -\epsilon_j z F_{\beta_j + \epsilon_j}(z) + \delta^{(J)}(sm_a \pm \sqrt{z^2 + m_a^2}) F_{\beta_j}(z), \quad F = J, Y, \end{aligned} \quad (2.15)$$

and $m_a = ma$. In the E-region $J = E$ and the notation for the I-region with $J = I$ is used below. Note that one has

$$g_{\beta_j, \beta_j}^{(\pm)}(\gamma a, \gamma a) = \frac{2}{\pi}, \quad g_{\beta_j, \beta_j + \epsilon_j}^{(\pm)}(\gamma a, \gamma a) = \delta^{(J)} \frac{2\epsilon_j}{\pi\gamma} \left(sm \pm \sqrt{\gamma^2 + m^2} \right). \quad (2.16)$$

In the E-region the mode functions (2.10) with $Z_\nu^{(\pm)}(\gamma r) = g_{\beta_j, \nu}^{(\pm)}(\gamma a, \gamma r)$ obey the boundary condition (2.8) and the spectrum of the quantum number γ is continuous, $0 \leq \gamma < \infty$. For the I-region the eigenvalues of γ are quantized by the boundary condition. They are solutions of the equation

$$\bar{J}_{\beta_j}^{(\pm)}(\gamma a) = 0. \quad (2.17)$$

We denote the positive roots of this equation by $\gamma a = \gamma_{j,l}^{(\pm)}$, $l = 1, 2, \dots$. Hence, in the I-region the modes are specified by the set $\sigma = (l, j)$.

The mode functions (2.10) are normalized by the condition

$$\int_0^{\phi_0} d\phi \int dr r \bar{\psi}_\sigma^{(\pm)} \gamma^0 \psi_{\sigma'}^{(\pm)} = \delta_{\sigma\sigma'}, \quad (2.18)$$

where $\bar{\psi} = \psi^\dagger \gamma^0$ is the Dirac adjoint and the radial integration goes over $[0, a]$ and $[a, \infty)$ for the I- and E-regions. One has $\delta_{\sigma\sigma'} = \delta_{ll'} \delta_{jj'}$ and $\delta_{\sigma\sigma'} = \delta(\gamma - \gamma') \delta_{jj'}$ in those regions, respectively. For the normalization coefficient in the I-region one finds

$$|c^{(\pm)}|^2 \equiv |c_i^{(\pm)}|^2 = \frac{\gamma}{2\phi_0 a} \frac{E \pm sm}{E} T_{\beta_j}^{(\pm)}(\gamma a), \quad (2.19)$$

where we have defined

$$T_{\beta_j}^{(\pm)}(z) = \frac{z J_{\beta_j}^{-2}(z)}{a(E \pm sm) [aE \mp q(j + \alpha_0) + \frac{sm}{2E}]}, \quad (2.20)$$

with $E = \sqrt{z^2/a^2 + m^2}$ and $z = \gamma_{j,l}^{(\pm)}$. For the E-region we get

$$|c^{(\pm)}|^2 \equiv |c_e^{(\pm)}|^2 = \frac{\gamma}{2\phi_0 E} \frac{E \pm sm}{\bar{J}_{\beta_j}^{(\pm)2}(\gamma a) + \bar{Y}_{\beta_j}^{(\pm)2}(\gamma a)}. \quad (2.21)$$

Note that the mode functions in the boundary-free conical space with $0 \leq r < \infty$ are given by (2.10) with $Z_\nu^{(\pm)}(\gamma r) = J_\nu(\gamma r)$. The corresponding normalization coefficient is found from (2.18) with the radial integration over $[0, \infty)$. This gives

$$|c^{(\pm)}|^2 \equiv |c_0^{(\pm)}|^2 = \gamma \frac{E \pm sm}{2\phi_0 E}. \quad (2.22)$$

We turn to the evaluation of the expectation values of the charge and current densities for the field $\psi(x)$ in thermal equilibrium at temperature T . They are expressed in terms of the density matrix $\hat{\rho} = e^{-\beta(\hat{H} - \mu' \hat{Q})}/Z$, with $\beta = 1/T$, by the formula

$$\langle j^\nu \rangle = e \text{tr} [\hat{\rho} \bar{\psi} \gamma^\nu \psi], \quad \nu = 0, 1, 2, \quad (2.23)$$

where the angular brackets stand for the ensemble average. Here, $\hat{H} = \sum_\sigma E_\sigma (a_\sigma^\dagger a_\sigma - b_\sigma^\dagger b_\sigma)$ is the Hamilton operator, $\hat{Q} = e \sum_\sigma (a_\sigma^\dagger a_\sigma + b_\sigma^\dagger b_\sigma)$ is the charge operator and $Z = \text{tr} [e^{-\beta(\hat{H} - \mu' \hat{Q})}]$ is the partition function with the related chemical potential μ' .

Plugging in (2.23) the expansion (2.9) of the operator $\psi(x)$ and the corresponding expansion for the Dirac adjoint, the mean current density is presented in the form

$$\langle j^\nu \rangle = \langle j^\nu \rangle_{\text{vac}} + \langle j^\nu \rangle_{T+} + \langle j^\nu \rangle_{T-}, \quad (2.24)$$

where $\langle j^\nu \rangle_{\text{vac}}$ is the vacuum expectation value (VEV), $\langle j^\nu \rangle_{T+}$ and $\langle j^\nu \rangle_{T-}$ are the contributions coming from particles and antiparticles, respectively. Introducing the notation $\mu = e\mu'$, the separate contributions are given by the following expansions over the mode functions:

$$\langle j^\nu \rangle_{\text{vac}} = -\frac{e}{2} \sum_{\sigma} \sum_{\lambda=\pm} \lambda \bar{\psi}_{\sigma}^{(\lambda)}(x) \gamma^\nu \psi_{\sigma}^{(\lambda)}(x), \quad (2.25)$$

$$\langle j^\nu \rangle_{T\pm} = \pm e \sum_{\sigma} \frac{\bar{\psi}_{\sigma}^{(\pm)}(x) \gamma^\nu \psi_{\sigma}^{(\pm)}(x)}{e^{\beta(E_\sigma \mp \mu)} + 1}. \quad (2.26)$$

Here, $\sum_{\sigma} = \sum_j \sum_{l=1}^{\infty}$ in the I-region and $\sum_{\sigma} = \sum_j \int_0^{\infty} d\gamma$ for the E-region with $\sum_j = \sum_{j=\pm 1/2, \pm 3/2, \dots}$. We emphasize again that the part (2.25) corresponds to the VEV in the geometry with the boundary at $r = a$. It has been investigated in [31] (see also [26] for a conical ring with two circular boundaries). The thermal contributions (2.26) generally vanishes in the limit $T \rightarrow 0$ except when $|\mu| > m$ in which case $\langle j^\nu \rangle_{T+}$ (for $\mu > 0$) or $\langle j^\nu \rangle_{T-}$ (for $\mu < 0$) do not vanish at $T = 0$ as will be discussed later. If we present the parameter α in the form

$$\alpha = \alpha_0 + n_0, \quad |\alpha_0| < 1/2, \quad (2.27)$$

with n_0 being an integer, then, redefining $j + n_0 \rightarrow j$ in the series over j , we see that the expectation values (2.25) and (2.26) do not depend on the integer part. In terms of the magnetic flux this means that only the fractional part of the ratio of the magnetic flux and flux quantum is physically relevant.

Hence, in the discussion below, without loss of generality, we can take $\alpha_j = q|j + \alpha_0|$. It can be checked that under the replacements $\alpha_0 \rightarrow -\alpha_0$ and $j \rightarrow -j$ we have $\beta_j \rightleftarrows \beta_j + \epsilon_j$ and

$$\bar{F}_{\beta_j}^{(\pm)}(\gamma a) \rightarrow b(\gamma) \bar{F}_{\beta_j}^{(\mp)}(z), \quad g_{\beta_j, \beta_j}^{(\pm)}(\gamma a, \gamma r) \rightarrow b(\gamma) g_{\beta_j, \beta_j + \epsilon_j}^{(\mp)}(\gamma a, \gamma r), \quad (2.28)$$

with $b(\gamma) = -\delta^{(J)} \epsilon_j (sm \pm E)/\gamma$. From the second relation in (2.28) it follows that $g_{\beta_j, \beta_j + \epsilon_j}^{(\pm)}(\gamma a, \gamma r) \rightarrow b(\gamma) g_{\beta_j, \beta_j}^{(\mp)}(\gamma a, \gamma r)$. For the radial modes in the I-region one has $\gamma a = \gamma_{j,l}^{(\pm)}(\alpha_0)$. Now, by using the first relation in (2.28), we see that $\gamma_{-j,l}^{(-)}(-\alpha_0) = \gamma_{j,l}^{(+)}(\alpha_0)$. This gives the relation between the eigenmodes for particles and antiparticles.

3 Vacuum expectation values and thermal contributions in a conical space without boundary

For further convenience, in this section we summarize the results for the VEVs in a conical space with a circular boundary and for the finite temperature charge and current densities in a conical space with no boundaries. The total current density in the problem under consideration is presented in the form

$$\langle j^\nu \rangle = \langle j^\nu \rangle^{(0)} + \langle j^\nu \rangle^{(b)}, \quad (3.1)$$

where $\langle j^\nu \rangle^{(0)}$ is the term independent of the boundary at $r = a$. This term is decomposed into the vacuum and thermal contributions as

$$\langle j^\nu \rangle^{(0)} = \langle j^\nu \rangle_{\text{vac}}^{(0)} + \langle j^\nu \rangle_T^{(0)}. \quad (3.2)$$

The terms with superscript (b) depend explicitly on the boundary at $r = a$ and are decomposed as

$$\langle j^\nu \rangle^{(b)} = \langle j^\nu \rangle_{\text{vac}}^{(b)} + \langle j^\nu \rangle_T^{(b)}. \quad (3.3)$$

This Section computes $\langle j^\nu \rangle_{\text{vac}}^{(0)}$, $\langle j^\nu \rangle_{\text{vac}}^{(b)}$, and $\langle j^\nu \rangle_T^{(0)}$ in that order. Section 4 computes $\langle j^\nu \rangle_T^{(b)}$ in the region $r > a$. The part $\langle j^\nu \rangle_T^{(b)}$ in the region $r < a$ is evaluated in Section 5. The radial current density always vanishes: $\langle j^1 \rangle = 0$ and the remainder of the text will only concern $\nu = 0, 2$.

The boundary-independent part of the VEV for $\nu = 0, 2$ is given by

$$\begin{aligned} \langle j^\nu \rangle_{\text{vac}}^{(0)} = & -\frac{e}{2\pi r} \left\{ \sum_{l=1}^{[q/2]}' (-1)^l \sin(2\pi l \alpha_0) f_\nu(2mr \sin(\pi l/q)) \right. \\ & \left. - \frac{q}{\pi} \int_0^\infty dy \frac{f_\nu(2mr \cosh y) f(q, \alpha_0, y)}{\cosh(2qy) - \cos(q\pi)} \right\}, \end{aligned} \quad (3.4)$$

where the functions for the charge and azimuthal current densities are defined as

$$\begin{aligned} f_0(z) &= sme^{-z}, \quad f_2(z) = 2m^2 e^{-z} \frac{1+z}{z^2}, \\ f(q, \alpha_0, y) &= \sum_{\chi=\pm 1} \chi \cos[q\pi(1/2 - \chi\alpha_0)] \cosh[q(1 + 2\chi\alpha_0)y]. \end{aligned} \quad (3.5)$$

The square brackets in the upper limit of the summation in (3.4) mean the integer part of the enclosed expression and the prime means that for even q the term with $l = q/2$ should be taken with a coefficient 1/2. Note that in [31] the negative energy modes have been used with α replaced by $-\alpha$ and as a consequence of that the VEV (3.4) differ from the corresponding formula in [31] by the sign (see also [26]). For the magnetic flux equal to an integer number of magnetic flux quanta we have $\alpha_0 = 0$ and both the charge and current densities in (3.4) vanish. The VEV $\langle j^\nu \rangle_{\text{vac}}^{(0)}$ is an odd periodic function of the magnetic flux Φ with the period of flux quantum. From (3.4) it follows that [31]

$$\begin{aligned} \lim_{\alpha_0 \rightarrow \pm 1/2} \langle j^0 \rangle_{\text{vac}}^{(0)} &= \pm \frac{eqm}{2\pi^2 r} K_0(2mr), \\ \lim_{\alpha_0 \rightarrow \pm 1/2} \langle j^2 \rangle_{\text{vac}}^{(0)} &= \pm \frac{eqm}{2\pi^2 r^2} K_1(2mr). \end{aligned} \quad (3.6)$$

This shows that the VEVs $\langle j^\nu \rangle_{\text{vac}}^{(0)}$, considered as functions of α are discontinuous at the points $\alpha = n_0 + 1/2$ with n_0 being an integer. For a massless field the charge density $\langle j^0 \rangle_{\text{vac}}^{(0)}$ vanishes and the expression for the current density $\langle j^2 \rangle_{\text{vac}}^{(0)}$ is obtained from (3.4) by the replacement $f_2(2mr b) \rightarrow 1/(2r^2 b^2)$.

For a conical space with a circular edge the boundary-induced contributions in the VEVs are expressed as [26, 31]

$$\begin{aligned} \langle j^\nu \rangle_{\text{vac}}^{(\text{b})} &= \frac{e}{\pi \phi_0} \sum_j \int_m^\infty dx x \text{Re} \left[\frac{\bar{I}_{\beta_j}(ax)}{\bar{K}_{\beta_j}(ax)} \frac{U_{\nu, \beta_j}^K(rx)}{\sqrt{x^2 - m^2}} \right], \quad r > a, \\ \langle j^\nu \rangle_{\text{vac}}^{(\text{b})} &= \frac{e}{\pi \phi_0} \sum_j \int_m^\infty dx x \text{Re} \left[\frac{\bar{K}_{\beta_j}(ax)}{\bar{I}_{\beta_j}(ax)} \frac{U_{\nu, \beta_j}^I(rx)}{\sqrt{x^2 - m^2}} \right], \quad r < a, \end{aligned} \quad (3.7)$$

with $\nu = 0$ and $\nu = 2$ for the charge and azimuthal current densities¹. Here, for the modified Bessel functions $I_{\beta_j}(z)$ and $K_{\beta_j}(z)$ we use the notation

$$\begin{aligned} \bar{F}_{\beta_j}(u) &= u F'_{\beta_j}(u) - \left[\epsilon_j \beta_j - \delta^{(\text{J})} \left(sm_a + i\sqrt{u^2 - m_a^2} \right) \right] F_{\beta_j}(u) \\ &= \delta_F u F_{\beta_j + \epsilon_j}(u) + \delta^{(\text{J})} \left(sm_a + i\sqrt{u^2 - m_a^2} \right) F_{\beta_j}(u), \end{aligned} \quad (3.8)$$

¹As it has been mentioned in [26], comparing the expressions for the charge and current densities given here and in [26] with the corresponding expressions in [31], the parameters α and α_0 should be replaced by $-\alpha$ and $-\alpha_0$, respectively. The change of the signs is related to the fact that the negative energy mode functions used in [31] differ from those here by the sign of α .

where $F = I, K$, $\delta_I = -\delta_K = 1$ and $\delta^{(J)}$ is defined by (2.7). In (3.7) we have defined

$$\begin{aligned} U_{0,\beta_j}^F(rx) &= \sum_{\chi=\pm 1} \left(sm + \chi i \sqrt{x^2 - m^2} \right) F_{\alpha_j - \chi \epsilon_j/2}^2(rx), \\ U_{2,\beta_j}^F(rx) &= -\delta_F \frac{2x}{r} F_{\beta_j}(rx) F_{\beta_j + \epsilon_j}(rx), \end{aligned} \quad (3.9)$$

for the modified Bessel functions $F = I$ and $F = K$. It can be seen that under the replacement $\alpha_0 \rightarrow -\alpha_0$ and $j \rightarrow -j$ we have

$$\frac{\bar{I}_{\beta_j}(ax)}{\bar{K}_{\beta_j}(ax)} \rightarrow - \left[\frac{\bar{I}_{\beta_j}(ax)}{\bar{K}_{\beta_j}(ax)} \right]^*, \quad U_{2,\beta_j}^F(rx) \rightarrow U_{2,\beta_j}^{F*}(rx), \quad (3.10)$$

where the star stands for the complex conjugate. From these relations it follows that

$$\langle j^\nu \rangle_{\text{vac}}^{(b)}(-\alpha_0) = -\langle j^\nu \rangle_{\text{vac}}^{(b)}(\alpha_0). \quad (3.11)$$

In particular, for a magnetic flux taking integer multiple values of flux quantum one has $\alpha_0 = 0$ and the boundary-induced VEVs vanish, $\langle j^\nu \rangle_{\text{vac}}^{(b)} = 0$. Note that the VEV (3.4) in the geometry without boundary is also an odd function of α_0 .

In a conical space without boundaries the current density is decomposed as (3.2) where the vacuum part is given by (3.4) and for the thermal part one has

$$\begin{aligned} \langle j^0 \rangle_T^{(0)} &= \frac{e}{2\phi_0} \int_0^\infty d\gamma \gamma \sum_{\chi=\pm 1} \frac{\sinh(\beta\mu) + \chi sm \cosh(\beta\mu)/E}{\cosh(\beta E) + \cosh(\beta\mu)} \sum_j J_{\alpha_j - \chi \epsilon_j/2}^2(\gamma r), \\ \langle j^2 \rangle_T^{(0)} &= \frac{e}{r\phi_0} \cosh(\beta\mu) \int_0^\infty d\gamma \frac{\gamma^2 \sum_j \epsilon_j J_{\beta_j}(\gamma r) J_{\beta_j + \epsilon_j}(\gamma r)}{E \cosh(\beta E) + \cosh(\beta\mu)}. \end{aligned} \quad (3.12)$$

These formulas are obtained by the transformations of the corresponding expressions from [34]. Alternative representations for the thermal parts $\langle j^\nu \rangle_T^{(0)}$ having a structure similar to (3.4) can be found in [34]. Note that the physical azimuthal component of the current density is expressed in terms of the contravariant component $\langle j^2 \rangle$ by the relation

$$\langle j_\phi \rangle = r \langle j^2 \rangle. \quad (3.13)$$

In all formulas below the index $\nu = 0, 2$ of the current density j^ν stands for the contravariant components. From (3.12) we can see that

$$\langle j^\nu \rangle_T^{(0)}(-\alpha_0, -\mu) = -\langle j^\nu \rangle_T^{(0)}(\alpha_0, \mu). \quad (3.14)$$

Now, by taking into account that the azimuthal component is an even function of the chemical potential, we conclude that for the magnetic flux equal to an integer multiple of flux quantum ($\alpha_0 = 0$) one gets $\langle j^2 \rangle_T^{(0)} = 0$. The expression for the charge density in this case is simplified to

$$\langle j^0 \rangle_T^{(0)} = \frac{e}{\phi_0} \sinh(\beta\mu) \sum_{j>0} \int_0^\infty d\gamma \gamma \frac{J_{qj-1/2}^2(\gamma r) + J_{qj+1/2}^2(\gamma r)}{\cosh(\beta E) + \cosh(\beta\mu)}, \quad (3.15)$$

and it vanishes for a zero chemical potential. In the special case $\phi_0 = 2\pi$, the formulas given in this section describe the combined effects of the finite temperature, magnetic flux and concentric circular edge on the mean charge and current densities in (2+1)-dimensional Minkowski spacetime. In the simplest case of the absence of the magnetic flux and boundary the current density vanishes and the distribution of the charge is uniform with

$$\langle j^0 \rangle^{(0)} = \langle j^0 \rangle_T^{(0)} = \frac{e}{2\pi} \int_m^\infty dx \frac{\sinh(\beta\mu) x}{\cosh(\beta x) + \cosh(\beta\mu)}. \quad (3.16)$$

In the zero temperature limit this gives

$$\lim_{T \rightarrow 0} \langle j^0 \rangle^{(0)} = \text{sgn}(\mu) e \frac{\mu^2 - m^2}{4\pi} \theta(|\mu| - m), \quad (3.17)$$

with $\theta(x)$ being the Heaviside step function.

In the discussion below we are interested in the finite temperature parts $\langle j^\nu \rangle_{T\pm}$ for the geometry of a conical space with a circular edge. Those parts in the E- and I-regions will be considered separately.

4 Charge and current densities in the E-region

This section will compute $\langle j^\nu \rangle_T^{(b)}$ in the region $r > a$. The corresponding mode functions are given by (2.10) with $Z_\nu^{(\pm)}(\gamma r) = g_{\beta_j, \nu}^{(\pm)}(\gamma a, \gamma r)$. With those modes the thermal contributions to the charge density and azimuthal current density are given by

$$\begin{aligned} \langle j^0 \rangle_{T\pm} &= \frac{\pm e}{2\phi_0} \sum_j \int_0^\infty d\gamma \frac{\gamma}{E} \frac{\sum_{\chi=\pm 1} (E \pm \chi s m) g_{\beta_j, \alpha_j - \chi \epsilon_j / 2}^{(\pm)2}(\gamma a, \gamma r)}{[e^{\beta(E \mp \mu)} + 1] [\bar{J}_{\beta_j}^{(\pm)2}(\gamma a) + \bar{Y}_{\beta_j}^{(\pm)2}(\gamma a)]}, \\ \langle j^2 \rangle_{T\pm} &= \frac{e}{\phi_0 r} \sum_j \int_0^\infty d\gamma \frac{\epsilon_j \gamma^2 / E}{e^{\beta(E \mp \mu)} + 1} \frac{g_{\beta_j, \beta_j}^{(\pm)}(\gamma a, \gamma r) g_{\beta_j, \beta_j + \epsilon_j}^{(\pm)}(\gamma a, \gamma r)}{\bar{J}_{\beta_j}^{(\pm)2}(\gamma a) + \bar{Y}_{\beta_j}^{(\pm)2}(\gamma a)}. \end{aligned} \quad (4.1)$$

The radial component of the current density vanishes. As expected, the ratio $\langle j^0 \rangle_{T\pm} / e$ is positive for particles and negative for antiparticles. Considering the expectation values as functions of the parameters α_0 and μ , $\langle j^\nu \rangle_{T\pm} = \langle j^\nu \rangle_{T\pm}(\alpha_0, \mu)$, and by using the transformations (2.28) under the replacements $\alpha_0 \rightarrow -\alpha_0$ and $j \rightarrow -j$, the following relation is obtained between the current densities of particles and antiparticles:

$$\langle j^\nu \rangle_{T\pm}(-\alpha_0, -\mu) = -\langle j^\nu \rangle_{T\mp}(\alpha_0, \mu). \quad (4.2)$$

From this relation, for the thermal part of the total current density we get

$$\langle j^\nu \rangle_T(-\alpha_0, -\mu) = -\langle j^\nu \rangle_T(\alpha_0, \mu). \quad (4.3)$$

As it has been discussed in the previous section, the same relation takes place for the VEVs. Another simple relation between the physical components on the boundary $r = a$ follows from Eq. (2.16):

$$\langle j^0 \rangle_{T\pm} = -\langle j_\phi \rangle_{T\pm} = \frac{4e}{\pi^2 \phi_0} \sum_j \int_0^\infty d\gamma \frac{\gamma (sm/E \pm 1)}{e^{\beta(E \mp \mu)} + 1} \frac{1}{\bar{J}_{\beta_j}^{(\pm)2}(\gamma a) + \bar{Y}_{\beta_j}^{(\pm)2}(\gamma a)}. \quad (4.4)$$

This relation for the charge and current densities on the edge is a consequence of the boundary condition (2.8) and has been mentioned for the VEVs in other geometries in [26, 46, 47].

The finite temperature charge and current densities in the boundary-free geometry were studied in [34] and here we are interested in the boundary-induced effects. In order to extract those contributions we subtract from the expectation values (4.1) the corresponding quantities in the boundary-free conical space, denoted here by $\langle j^\nu \rangle_{T\pm}^{(0)}$. The expressions for the latter are obtained from (4.1) by the replacement

$$\frac{g_{\beta_j, \rho}^{(\pm)}(\gamma a, \gamma r)}{\sqrt{\bar{J}_{\beta_j}^{(\pm)2}(\gamma a) + \bar{Y}_{\beta_j}^{(\pm)2}(\gamma a)}} \rightarrow J_\rho(\gamma r), \quad (4.5)$$

with $\rho = \beta_j, \beta_j + \epsilon_j$.

For the further transformation of the boundary-induced part $\langle j^\nu \rangle_{T\pm}^{(b)} = \langle j^\nu \rangle_{T\pm} - \langle j^\nu \rangle_{T\pm}^{(0)}$, we use the identity

$$\frac{g_{\beta_j, \mu}^{(\pm)}(x, y) g_{\beta_j, \rho}^{(\pm)}(x, y)}{\bar{J}_{\beta_j}^{(\pm)2}(x) + \bar{Y}_{\beta_j}^{(\pm)2}(x)} - J_\mu(y) J_\rho(y) = -\frac{1}{2} \sum_{l=1,2} \frac{\bar{J}_{\beta_j}^{(\pm)}(x)}{\bar{H}_{\beta_j}^{(\pm, l)}(x)} H_\mu^{(l)}(y) H_\rho^{(l)}(y), \quad (4.6)$$

where $H_\mu^{(l)}(x)$ are the Hankel functions and $\mu, \rho = \beta_j, \beta_j + \epsilon_j$. Here, the notation with the bar for the Hankel functions is defined in accordance with (2.15). The boundary-induced contributions are presented in the form

$$\begin{aligned} \langle j^0 \rangle_{T\lambda}^{(b)} &= -\frac{\lambda e}{4\phi_0} \sum_j \sum_{l=1,2} \int_0^\infty d\gamma \frac{\gamma \bar{J}_{\beta_j}^{(\lambda)}(\gamma a)}{E \bar{H}_{\beta_j}^{(l, \lambda)}(\gamma a)} \frac{\sum_{\chi=\pm 1} (E + \lambda \chi s m) H_{\alpha_j - \chi \epsilon_j/2}^{(l)2}(\gamma r)}{e^{\beta(E - \lambda \mu)} + 1}, \\ \langle j^2 \rangle_{T\lambda}^{(b)} &= -\frac{e}{2\phi_0 r} \sum_j \sum_{l=1,2} \int_0^\infty d\gamma \frac{\epsilon_j \gamma^2 \bar{J}_{\beta_j}^{(\lambda)}(\gamma a)}{E \bar{H}_{\beta_j}^{(l, \lambda)}(\gamma a)} \frac{H_{\beta_j}^{(l)}(\gamma r) H_{\beta_j + \epsilon_j}^{(l)}(\gamma r)}{e^{\beta(E - \lambda \mu)} + 1}, \end{aligned} \quad (4.7)$$

with $\lambda = \pm$. The cases of $\mu \neq 0$ and $\mu = 0$ will be discussed separately.

For the case of nonzero chemical potential, after transformations presented in Appendix A, for the expectation values of the charge and current densities coming from particles and antiparticles we get

$$\begin{aligned} \langle j^0 \rangle_{T\lambda}^{(b)} &= \frac{e}{\pi \phi_0} \sum_j \left\{ - \int_m^\infty dx x \operatorname{Re} \left[\frac{\bar{I}_{\beta_j}(xa)}{\bar{K}_{\beta_j}(xa)} \frac{U_{0, \beta_j}^K(xr)}{\sqrt{x^2 - m^2}} \frac{1}{e^{\lambda \beta(i\sqrt{x^2 - m^2} - \mu)} + 1} \right] \right. \\ &\quad \left. + 2\pi T \theta(\lambda \mu) \sum_{n=0}^\infty \operatorname{Re} \left[\frac{\bar{I}_{\beta_j}(u_n a)}{\bar{K}_{\beta_j}(u_n a)} \sum_{\chi=\pm 1} [sm + \chi \mu + \chi i \pi (2n+1) T] K_{\alpha_j - \chi \epsilon_j/2}^2(u_n r) \right] \right\}, \\ \langle j^2 \rangle_{T\lambda}^{(b)} &= \frac{e}{\pi \phi_0} \sum_j \left\{ - \int_m^\infty dx \frac{x U_{2, \beta_j}^K(xr)}{\sqrt{x^2 - m^2}} \operatorname{Re} \left[\frac{\bar{I}_{\beta_j}(xa)}{\bar{K}_{\beta_j}(xa)} \frac{1}{e^{\lambda \beta(i\sqrt{x^2 - m^2} - \mu)} + 1} \right] \right. \\ &\quad \left. + 2\pi T \theta(\lambda \mu) \sum_{n=0}^\infty \operatorname{Re} \left[\frac{\bar{I}_{\beta_j}(u_n a)}{\bar{K}_{\beta_j}(u_n a)} U_{2, \beta_j}^K(u_n r) \right] \right\}, \end{aligned} \quad (4.8)$$

where

$$u_n = \left\{ [\pi (2n+1) T - i\mu]^2 + m^2 \right\}^{1/2}. \quad (4.9)$$

We have also used the notation $\bar{F}_{\beta_j}(z) = \bar{F}_{\beta_j}^{(+)}(z)$ for the modified Bessel functions in agreement with (3.8) where $\delta^{(J)} = \delta^{(E)} = -1$.

By combining the contributions from the separate terms with $\lambda = +$ and $\lambda = -$ and using the identity $\sum_\lambda 1/(e^{\lambda z} + 1) = 1$, we obtain the boundary-induced finite temperature contributions $\langle j^\nu \rangle_T^{(b)} = \sum_{\lambda=\pm} \langle j^\nu \rangle_{T\lambda}^{(b)}$. Afterwards, the total boundary-induced contributions, given by the formula (3.3) are presented in the form

$$\begin{aligned} \langle j^0 \rangle^{(b)} &= \frac{2Te}{\phi_0} \sum_j \sum_{n=0}^\infty \operatorname{Re} \left\{ \frac{\bar{I}_{\beta_j}(u_n a)}{\bar{K}_{\beta_j}(u_n a)} \sum_{\chi=\pm 1} [sm + \chi \mu + \chi i \pi (2n+1) T] K_{\alpha_j - \chi \epsilon_j/2}^2(u_n r) \right\}, \\ \langle j^2 \rangle^{(b)} &= \frac{2Te}{\phi_0} \sum_j \sum_{n=0}^\infty \operatorname{Re} \left[\frac{\bar{I}_{\beta_j}(u_n a)}{\bar{K}_{\beta_j}(u_n a)} U_{2, \beta_j}^K(u_n r) \right], \end{aligned} \quad (4.10)$$

where the function $U_{2, \beta_j}^K(u_n r)$ is given by (3.9) with $F = K$ and the modified Bessel functions with bar are defined as (3.8) with $J = E$, $\delta^{(E)} = -1$. Introducing the functions

$$W_j^{(J)}(z) = \sum_{\chi=\pm 1} \chi \left[I_{\alpha_j - \chi \epsilon_j/2}(z) + \delta^{(J)} \frac{sm a}{z} I_{\alpha_j + \chi \epsilon_j/2}(z) \right] K_{\alpha_j - \chi \epsilon_j/2}(z), \quad (4.11)$$

with $J = I, E$ and $\delta^{(J)}$ defined as (2.7), the real parts in (A.4) are explicitly separated by using the relation

$$\frac{\bar{I}_{\beta_j}(z)}{\bar{K}_{\beta_j}(z)} = \frac{W_j^{(E)}(z) + [\mu + i\pi(2n+1)T]a/z^2}{K_{\beta_j+\epsilon_j}^2(z) + K_{\beta_j}^2(z) + 2sm_a K_{\beta_j}(z) K_{\beta_j+\epsilon_j}(z)/z}. \quad (4.12)$$

The function $W_j^{(I)}(z)$ will appear in the formulas below for the I-region. Note that under the replacement $\alpha_0 \rightarrow -\alpha_0$, $j \rightarrow -j$ we have $W_j^{(J)}(z) \rightarrow -W_j^{(J)}(z)$.

In the case of zero chemical potential, $\mu = 0$, the poles of the integrand in (4.7) are located on the imaginary axis and the procedure for the transformation is different from that we have described above. This case is considered in Appendix A and the corresponding result is obtained from (4.10) by taking the limit $\mu \rightarrow 0$. For $\mu = 0$ in the arguments of the modified Bessel functions we have $u_n = u_{0n}$, with

$$u_{0n} = \sqrt{[\pi(2n+1)T]^2 + m^2}, \quad (4.13)$$

and the arguments are real. By taking into account (4.12) the real parts are explicitly separated and we get

$$\begin{aligned} \langle j^0 \rangle^{(b)} &= \frac{2Te}{a\phi_0} \sum_j \sum_{n=0}^{\infty} \sum_{\chi=\pm 1} \frac{\left[sm_a W_j^{(E)}(z) - \chi \left(1 - \frac{m_a^2}{z^2} \right) \right] K_{\alpha_j-\chi\epsilon_j/2}^2(zr/a)}{K_{\beta_j+\epsilon_j}^2(z) + K_{\beta_j}^2(z) + 2sm_a K_{\beta_j}(z) K_{\beta_j+\epsilon_j}(z)/z}, \\ \langle j^2 \rangle^{(b)} &= \frac{2Te}{\phi_0} \sum_j \sum_{n=0}^{\infty} \frac{W_j^{(E)}(z) U_{2,\beta_j}^K(zr/a)}{K_{\beta_j+\epsilon_j}^2(z) + K_{\beta_j}^2(z) + 2sm_a K_{\beta_j}(z) K_{\beta_j+\epsilon_j}(z)/z}, \end{aligned} \quad (4.14)$$

where $z = au_{0n}$. These expressions are further simplified for a massless field:

$$\begin{aligned} \langle j^0 \rangle^{(b)} &= \frac{2Te}{a\phi_0} \sum_j \sum_{n=0}^{\infty} \frac{K_{\beta_j+\epsilon_j}^2(zr/a) - K_{\beta_j}^2(zr/a)}{K_{\beta_j+\epsilon_j}^2(z) + K_{\beta_j}^2(z)}, \\ \langle j^2 \rangle^{(b)} &= \frac{2Te}{\phi_0} \sum_j \sum_{n=0}^{\infty} \sum_{\chi=\pm 1} \frac{\chi I_{\alpha_j-\chi\epsilon_j/2}(z) K_{\alpha_j-\chi\epsilon_j/2}(z)}{K_{\beta_j+\epsilon_j}^2(z) + K_{\beta_j}^2(z)} U_{2,\beta_j}^K(zr/a), \end{aligned} \quad (4.15)$$

with $z = (2n+1)\pi aT$. In this case the expectation values do not depend on the parameter s , as anticipated.

For $\mu = 0$ the zero temperature limit of the charge and current densities is directly obtained from (4.14) (or from (4.10) with $u_n = u_{0n}$) by taking into account that for small temperatures the dominant contribution comes from the terms with large n and one can replace the summation over n by the integration. This is reduced to the replacement

$$\sum_{n=0}^{\infty} f(u_{0n}) \rightarrow \frac{1}{2\pi T} \int_m^{\infty} dx \frac{xf(x)}{\sqrt{x^2 - m^2}}, \quad (4.16)$$

and we can see that the result (3.7) for $r > a$ is obtained.

Now, let us consider the charge and current densities in the zero temperature limit for $\mu \neq 0$. When discussing that limit, it is more convenient to use the representations (4.1). For $|\mu| < m$ we have $E > |\mu|$ in the entire range of γ -integration and the thermal contributions $\langle j^\nu \rangle_{T\pm}$ in the expectation values tend to zero. Consequently, the expectation values are reduced to the corresponding VEVs:

$$\langle j^\nu \rangle_{T=0} = \langle j^\nu \rangle_{\text{vac}}, \quad |\mu| < m. \quad (4.17)$$

The zero temperature limit is qualitatively different in the case $|\mu| > m$. In this range, the contributions from particles/antiparticles survive in the limit $T \rightarrow 0$. Those contributions come from the integration

range $\gamma \in [0, \gamma_F]$ with $\gamma_F = \sqrt{\mu^2 - m^2}$. The zero temperature mean charge and current densities are presented as

$$\begin{aligned}\langle j^0 \rangle_{T=0} &= \langle j^0 \rangle_{\text{vac}} + \frac{e}{2\phi_0} \sum_j \int_0^{\gamma_F} d\gamma \frac{\gamma}{E} \frac{\sum_{\chi=\pm 1} (\lambda E + \chi sm) g_{\beta_j, \alpha_j - \chi \epsilon_j / 2}^{(\lambda)2}(\gamma a, \gamma r)}{\bar{J}_{\beta_j}^{(\lambda)2}(\gamma a) + \bar{Y}_{\beta_j}^{(\lambda)2}(\gamma a)}, \\ \langle j^2 \rangle_{T=0} &= \langle j^2 \rangle_{\text{vac}} + \frac{e}{r\phi_0} \sum_j \epsilon_j \int_0^{\gamma_F} d\gamma \frac{\gamma^2}{E} \frac{g_{\beta_j, \beta_j}^{(\lambda)}(\gamma a, \gamma r) g_{\beta_j, \beta_j + \epsilon_j}^{(\lambda)}(\gamma a, \gamma r)}{\bar{J}_{\beta_j}^{(\lambda)2}(\gamma a) + \bar{Y}_{\beta_j}^{(\lambda)2}(\gamma a)},\end{aligned}\quad (4.18)$$

where λ is determined by the relation $\mu = \lambda|\mu|$. Hence, the zero temperature state contains particles for $\mu > m$ ($\lambda = +$) and antiparticles for $\mu < -m$ ($\lambda = -$). As expected, the sign of the ratio $(\langle j^0 \rangle_{T=0} - \langle j^0 \rangle_{\text{vac}})/e$ coincides with λ . Similarly, the zero temperature limit in the boundary-free geometry for the case $|\mu| > m$ is reduced to

$$\begin{aligned}\langle j^0 \rangle_{T=0}^{(0)} &= \langle j^0 \rangle_{\text{vac}}^{(0)} + \frac{e}{2\phi_0} \int_0^{\gamma_F} d\gamma \frac{\gamma}{E} \sum_{\chi=\pm 1} (\lambda E + \chi sm) \sum_j J_{\alpha_j - \chi \epsilon_j / 2}^2(\gamma r), \\ \langle j^2 \rangle_{T=0}^{(0)} &= \langle j^2 \rangle_{\text{vac}}^{(0)} + \frac{e}{r\phi_0} \int_0^{\gamma_F} d\gamma \frac{\gamma^2}{E} \sum_j \epsilon_j J_{\beta_j}(\gamma r) J_{\beta_j + \epsilon_j}(\gamma r),\end{aligned}\quad (4.19)$$

with the same choice of λ . The part of the integral in the expression (4.19) for the charge density containing λ is evaluated by using the formula from [48]. Note that in (4.19) the azimuthal current density is the same for particles and antiparticles. In Appendix B we show that the same zero temperature limit (4.18) is obtained starting from (4.10).

5 Charge and current densities in the I-region

In this section we consider the charge and current densities in the interior region, $r \leq a$. The substitution of mode functions (2.10) into the formula (2.26) gives

$$\langle j^\nu \rangle_{T\lambda} = \frac{\lambda e}{2\phi_0 a} \sum_j \sum_{l=1}^{\infty} \frac{T_{\beta_j}^{(\lambda)}(z) g^{(\nu)}(z/a)}{e^{\beta(E - \lambda\mu)} + 1}, \quad (5.1)$$

with $\nu = 0, 2$, $z = \gamma_{j,l}^{(\lambda)}$ being the positive roots of the equation (2.17), and $E = \sqrt{z^2/a^2 + m^2}$. As before, the expectation values with $\lambda = +$ and $\lambda = -$ present the contributions of the positive and negative energy modes. We have also introduced the functions

$$\begin{aligned}g^{(0)}(\gamma) &= \gamma \sum_{\chi=\pm 1} \left(1 + \frac{\chi \lambda sm}{\sqrt{\gamma^2 + m^2}} \right) J_{\alpha_j - \chi \epsilon_j / 2}^2(\gamma r), \\ g^{(2)}(\gamma) &= \lambda \epsilon_j \gamma^2 \frac{2 J_{\beta_j}(\gamma r) J_{\beta_j + \epsilon_j}(\gamma r)}{r \sqrt{\gamma^2 + m^2}}.\end{aligned}\quad (5.2)$$

for the charge and azimuthal current densities. The radial component of the current density vanishes. From (2.19) it follows that $T_{\beta_j}^{(\lambda)}(z) > 0$ and, hence, the sign of the ratio $\langle j^0 \rangle_{T\lambda}/e$ coincides with λ . Of course, this agrees with the interpretation of $\langle j^\nu \rangle_{T\lambda}$ as the contribution from particles for $\lambda = +$ and from antiparticles for $\lambda = -$. By using the fact that the eigenvalues $\gamma_{j,l}^{(\pm)}$ are the roots of the equation (2.17), it can be seen that under the replacements $\alpha_0 \rightarrow -\alpha_0$ and $j \rightarrow -j$ one has $T_{\beta_j}^{(\pm)}(\gamma_{j,l}^{(\pm)}) \rightarrow T_{\beta_j}^{(\mp)}(\gamma_{j,l}^{(\mp)})$. In combination with (5.2), this shows that the charge and current densities obey the relations (4.2) and

(4.3). In addition, the following relation takes place on the boundary $r = a$ (compare with (4.4) in the E-region):

$$\langle j^0 \rangle_{T\lambda} = \langle j_\phi \rangle_{T\lambda} = \frac{\lambda e}{\phi_0 a^2} \sum_j \sum_{l=1}^{\infty} \frac{u T_{\beta_j}^{(\lambda)}(z) J_{\beta_j}^2(z)}{e^{\beta(E-\lambda\mu)} + 1} \left(1 + \frac{\lambda s m}{E}\right), \quad (5.3)$$

with $z = \gamma_{j,l}^{(\lambda)}$.

The expressions for $\langle j^\nu \rangle_{T\lambda}$ given by (5.1) are not convenient for numerical analysis since the zeros $\gamma_{j,l}^{(\lambda)}$ are given implicitly. In addition, the terms with large values of l are highly oscillatory. We will transform the series over l in (5.1). That is done by using the generalized Abel-Plana formula [49, 50] for series $\sum_{l=1}^{\infty} T_{\beta_j}(\gamma_{j,l}^{(\lambda)}) f^{(\nu)}(\gamma_{j,l}^{(\lambda)})$ with the function $f^{(\nu)}(z)$ given by

$$f^{(\nu)}(z) = \frac{g^{(\nu)}(z/a)}{e^{\beta(\sqrt{z^2/a^2+m^2}-\lambda\mu)} + 1}, \quad (5.4)$$

for $\nu = 0, 2$.

Firstly, we discuss the case of $\mu \neq 0$. The functions (5.4) have branch points $z = \pm im_a$, corresponding to $E = 0$, and simple poles $z_n^{(\lambda)} = a\gamma_n^{(\lambda)}$, $n = 0, \pm 1, \pm 2, \dots$, at the zeros of the function $e^{\beta(E-\lambda\mu)} + 1$. These zeros correspond to the values of energy $E = E_n^{(\lambda)}$ with

$$E_n^{(\lambda)} = \lambda\mu + i\pi(2n+1)T, \quad (5.5)$$

and for them we have

$$\gamma_n^{(\lambda)2} = E_n^{(\lambda)2} - m^2, \quad (5.6)$$

with $n = 0, \pm 1, \pm 2, \dots$. One has $\text{Im}(z_n^{(\lambda)}) > 0$ for $n = 0, 1, 2, \dots$, and $\text{Im}(z_n^{(\lambda)}) < 0$ for $n = \dots, -2, -1$. For the real parts we have $\text{sgn}(\lambda\mu) \text{Re}(z_n^{(\lambda)}) > 0$. In addition, the relations $E_n^{(\lambda)} = E_{-n-1}^{(\lambda)*}$ and $\gamma_n^{(\lambda)} = \gamma_{-n-1}^{(\lambda)*}$, $n = \dots, -2, -1$, take place for the poles in the lower and upper half-planes. For $\lambda\mu > 0$ both functions $f^{(\nu)}(z)$ have simple poles in the right half-plane, $z = z_n^{(\lambda)} \equiv iau_n^{(\lambda)}$, $n = 0, \pm 1, \pm 2, \dots$, with

$$u_n^{(\lambda)} = \left\{ [\pi(2n+1)T - i\lambda\mu]^2 + m^2 \right\}^{1/2} \quad (5.7)$$

and $\text{Re}(au_n^{(\lambda)}) > 0$. Under these conditions we have the following summation formula [45]

$$\begin{aligned} \sum_{l=1}^{\infty} T_{\beta_j}^{(\lambda)}(\gamma_{j,l}^{(\lambda)}) f^{(\nu)}(\gamma_{j,l}^{(\lambda)}) &= \int_0^{\infty} dx f^{(\nu)}(x) + \frac{\pi}{2} \underset{z=0}{\text{Res}} \frac{\tilde{Y}_{\beta_j}^{(\lambda)}(z)}{\tilde{J}_{\beta_j}^{(\lambda)}(z)} f^{(\nu)}(z) \\ &\quad - 4 \sum_{n=0}^{\infty} \text{Re} \left[e^{-i\pi\beta_j} \frac{\tilde{K}_{\beta_j}^{(\lambda)}(u_n^{(\lambda)}a)}{\tilde{I}_{\beta_j}^{(\lambda)}(u_n^{(\lambda)}a)} \underset{z=z_n^{(\lambda)}}{\text{Res}} f^{(\nu)}(z) \right] \\ &\quad - \frac{2}{\pi} \int_0^{\infty} dx \text{Re} \left[e^{-i\pi\beta_j} f^{(\nu)}(xe^{\pi i/2}) \frac{\tilde{K}_{\beta_j}^{(\lambda)}(x)}{\tilde{I}_{\beta_j}^{(\lambda)}(x)} \right], \end{aligned} \quad (5.8)$$

with the notation

$$\tilde{F}_{\beta_j}^{(\lambda)}(x) = xF'_{\beta_j}(x) + [\delta^{(J)}(sm_a + \lambda\sqrt{(e^{\pi i/2}x)^2 + m_a^2}) - \epsilon_j\beta_j]F_{\beta_j}(x), \quad F = I, K, \quad (5.9)$$

for the modified Bessel functions. We consider the I-region and in (5.9) $\delta^{(J)} = \delta^{(I)} = 1$. The notation with $J = E$ is used in the transformation of the expectation values for the E-region, given in Appendix A. The contribution of the first term in the right-hand side of (5.8) gives the expectation value in the

boundary-free conical space. Denoting the latter for the modes with $\lambda = +$ and $\lambda = -$ by $\langle j^\nu \rangle_{T\lambda}^{(0)}$ and introducing a new integration variable $\gamma = x/a$, we have

$$\langle j^\nu \rangle_{T\lambda}^{(0)} = \frac{\lambda e}{2\phi_0} \sum_j \int_0^\infty d\gamma \frac{g^{(\nu)}(\gamma)}{e^{\beta(\sqrt{\gamma^2+m^2}-\lambda\mu)} + 1}. \quad (5.10)$$

Of course, this part does not depend on a . As it has been already mentioned before, the expression (5.10) for the boundary-free geometry is obtained from the expressions (4.1) for the E-region by the replacement (4.5). It can be checked that the combined thermal current density $\sum_{\lambda=\pm} \langle j^\nu \rangle_{T\lambda}^{(0)}$, with $\langle j^\nu \rangle_{T\lambda}^{(0)}$ from (5.10), is transformed to (3.12).

For the function (5.4) the term in (5.8) with the residue at $z = 0$ and the part of the last integral over the region $x \in [0, ma]$ become zero. Note that in the region $x \in [ma, \infty)$ we have

$$\tilde{F}_{\beta_j}^{(+)}(x) = [\tilde{F}_{\beta_j}^{(-)}(x)]^* = \bar{F}_{\beta_j}(x). \quad (5.11)$$

By using this property, the thermal contributions are presented in the form

$$\langle j^\nu \rangle_{T\lambda} = \langle j^\nu \rangle_{T\lambda}^{(0)} + \langle j^\nu \rangle_{T\lambda}^{(b)}, \quad (5.12)$$

where the boundary-induced parts are expressed as

$$\begin{aligned} \langle j^0 \rangle_{T\lambda}^{(b)} &= \frac{e}{\pi\phi_0} \sum_j \sum_{\chi=\pm 1} \left\{ - \int_m^\infty dx x \operatorname{Re} \left[\frac{\tilde{K}_{\beta_j}^{(\lambda)}(xa)}{\tilde{I}_{\beta_j}^{(\lambda)}(xa)} \frac{sm + \lambda\chi i\sqrt{x^2-m^2}}{e^{\beta(i\sqrt{x^2-m^2}-\lambda\mu)} + 1} \frac{I_{\alpha_j-\chi\epsilon_j/2}^2(xr)}{\sqrt{x^2-m^2}} \right] \right. \\ &\quad \left. + 2\pi T \theta(\lambda\mu) \sum_{n=0}^\infty \operatorname{Re} \left[\frac{\tilde{K}_{\beta_j}^{(\lambda)}(u_n^{(\lambda)}a)}{\tilde{I}_{\beta_j}^{(\lambda)}(u_n^{(\lambda)}a)} [sm + \chi\mu + \lambda i\chi\pi(2n+1)T] I_{\alpha_j-\chi\epsilon_j/2}^2(u_n^{(\lambda)}r) \right] \right\}, \\ \langle j^2 \rangle_{T\lambda}^{(b)} &= \frac{e}{\pi\phi_0} \sum_j \left\{ - \int_m^\infty dx \frac{x U_{2,\beta_j}^I(xr)}{\sqrt{x^2-m^2}} \operatorname{Re} \left[\frac{\tilde{K}_{\beta_j}^{(\lambda)}(xa)}{\tilde{I}_{\beta_j}^{(\lambda)}(xa)} \frac{1}{e^{\beta(i\sqrt{x^2-m^2}-\lambda\mu)} + 1} \right] \right. \\ &\quad \left. + 2\pi T \theta(\lambda\mu) \sum_{n=0}^\infty \operatorname{Re} \left[\frac{\tilde{K}_{\beta_j}^{(\lambda)}(u_n^{(\lambda)}a)}{\tilde{I}_{\beta_j}^{(\lambda)}(u_n^{(\lambda)}a)} U_{2,\beta_j}^I(u_n^{(\lambda)}r) \right] \right\}. \end{aligned} \quad (5.13)$$

By using the relations (5.11) these expressions are transformed to

$$\begin{aligned} \langle j^0 \rangle_{T\lambda}^{(b)} &= \frac{e}{\pi\phi_0} \sum_j \left\{ - \int_m^\infty dx x \operatorname{Re} \left[\frac{\bar{K}_{\beta_j}(xa)}{\bar{I}_{\beta_j}(xa)} \frac{U_{0,\beta_j}^I(xr)}{\sqrt{x^2-m^2}} \frac{1}{e^{\lambda\beta(i\sqrt{x^2-m^2}-\mu)} + 1} \right] \right. \\ &\quad \left. + 2\pi T \theta(\lambda\mu) \sum_{n=0}^\infty \operatorname{Re} \left[\frac{\bar{K}_{\beta_j}(u_n a)}{\bar{I}_{\beta_j}(u_n a)} \sum_{\chi=\pm 1} [sm + \chi\mu + i\chi\pi(2n+1)T] I_{\alpha_j-\chi\epsilon_j/2}^2(u_n r) \right] \right\}, \\ \langle j^2 \rangle_{T\lambda}^{(b)} &= -\frac{e}{\pi\phi_0} \sum_j \left\{ \int_m^\infty dx \frac{x}{\sqrt{x^2-m^2}} \operatorname{Re} \left[\frac{\bar{K}_{\beta_j}(xa)}{\bar{I}_{\beta_j}(xa)} \frac{U_{2,\beta_j}^I(xr)}{e^{\lambda\beta(i\sqrt{x^2-m^2}-\mu)} + 1} \right] \right. \\ &\quad \left. - 2\pi T \theta(\lambda\mu) \sum_{n=0}^\infty \operatorname{Re} \left[\frac{\bar{K}_{\beta_j}(u_n a)}{\bar{I}_{\beta_j}(u_n a)} U_{2,\beta_j}^I(u_n r) \right] \right\}, \end{aligned} \quad (5.14)$$

where the notation with bar is defined by (3.8) with $J = I$ and $\delta^{(I)} = 1$ for the I-region.

By taking the sum of the currents for $\lambda = +$ and $\lambda = -$ and, again, using the relation $\sum_\lambda 1/(e^{\lambda z} + 1) = 1$, we see that the sum of the first terms in the figure braces of (5.14) gives $-\langle j^\nu \rangle_{\text{vac}}^{(b)}$ for both expectation

values (see Eq. (3.7)). As a consequence, the boundary-induced contributions $\langle j^\nu \rangle^{(b)}$, given by (3.3), take the form

$$\begin{aligned}\langle j^0 \rangle^{(b)} &= \frac{2eT}{\phi_0} \sum_j \sum_{n=0}^{\infty} \operatorname{Re} \left[\frac{\bar{K}_{\beta_j}(u_n a)}{\bar{I}_{\beta_j}(u_n a)} \sum_{\chi=\pm 1} [sm + \chi\mu + \chi i\pi(2n+1)T] I_{\alpha_j-\chi\epsilon_j/2}^2(u_n r) \right], \\ \langle j^2 \rangle^{(b)} &= \frac{2eT}{\phi_0} \sum_j \sum_{n=0}^{\infty} \operatorname{Re} \left[\frac{\bar{K}_{\beta_j}(u_n a)}{\bar{I}_{\beta_j}(u_n a)} U_{2,\beta_j}^I(u_n r) \right],\end{aligned}\quad (5.15)$$

where u_n is defined by (4.9). The total expectation values are presented as (3.1) with $\langle j^\nu \rangle^{(0)}$ having the form (3.2). For the ratio of the combinations of the modified Bessel functions in (5.15) we have the representation

$$\frac{\bar{K}_{\beta_j}(z)}{\bar{I}_{\beta_j}(z)} = \frac{W_j^{(I)}(z) + [\mu + i\pi(2n+1)T]a/z^2}{I_{\beta_j}^2(z) + I_{\beta_j+\epsilon_j}^2(z) + 2sm_a I_{\beta_j}(z) I_{\beta_j+\epsilon_j}(z)/z}, \quad (5.16)$$

where the function $W_j^{(I)}(z)$ is defined by (4.11) with $J = I$ and $\delta^{(I)} = 1$.

Now we consider the transformation of the thermal contributions $\langle j^\nu \rangle_{T\lambda}$ to the expectation values coming from particles and antiparticles given by (5.1) for the case of $\mu = 0$. The corresponding procedure for the evaluation of the boundary-induced part $\langle j^\nu \rangle^{(b)}$ differs from that we have described above for $\mu \neq 0$. Now, the poles of the functions $f^{(\nu)}(z)$, given by (5.4), are located on the imaginary axis. They are given as $z = \pm iau_{0n}$, $n = 0, 1, 2, \dots$, where u_{0n} is defined in accordance with (4.13). The Abel-Plana type summation formula adapted for this case is given in [45]. It is obtained from (5.8) by the replacement

$$\operatorname{Res}_{z=z_n^{(\lambda)}} f^{(\nu)}(z) \rightarrow \frac{1}{2} \operatorname{Res}_{z=iau_{0n}} f^{(\nu)}(z), \quad (5.17)$$

and by the replacement $\int_0^\infty dx \rightarrow \text{p.v.} \int_0^\infty dx$ in the last integral. Here, p.v. stands for the principal value of the integral. For $\mu = 0$ the term coming from the poles iau_{0n} is present for both $\lambda = +$ and $\lambda = -$, whereas in (5.8) the pole term is present only in the case of $\lambda\mu > 0$. Further transformations of the expectation values are similar to those for the E-region. In the region $r < a$, the expressions for $\langle j^0 \rangle_{T\lambda}^{(b)}$ and $\langle j^0 \rangle_T^{(b)}$ are obtained from (A.3) and (A.4) by the replacements $I \rightleftharpoons K$. For the expressions of $\langle j^2 \rangle_{T\lambda}^{(b)}$ and $\langle j^2 \rangle_T^{(b)}$ in the I-region, in addition to those replacements, the sign is changed. As a result, for the boundary-induced contributions we obtain

$$\begin{aligned}\langle j^0 \rangle^{(b)} &= \frac{2eT}{a\phi_0} \sum_j \sum_{n=0}^{\infty} \sum_{\chi=\pm 1} \frac{\left[sm_a W_j^{(I)}(z) - \chi \left(1 - \frac{m_a^2}{z^2} \right) \right] I_{\alpha_j-\chi\epsilon_j/2}^2(zr/a)}{I_{\beta_j}^2(z) + I_{\beta_j+\epsilon_j}^2(z) + 2sm_a I_{\beta_j}(z) I_{\beta_j+\epsilon_j}(z)/z}, \\ \langle j^2 \rangle^{(b)} &= \frac{2eT}{\phi_0} \sum_j \sum_{n=0}^{\infty} \frac{W_j^{(I)}(z) U_{2,\beta_j}^I(zr/a)}{I_{\beta_j}^2(z) + I_{\beta_j+\epsilon_j}^2(z) + 2sm_a I_{\beta_j}(z) I_{\beta_j+\epsilon_j}(z)/z}, \quad z = au_{0n}.\end{aligned}\quad (5.18)$$

We see that the expressions (5.18) for $\langle j^\nu \rangle^{(b)}$ are also directly obtained from (5.15) in the limit $\mu \rightarrow 0$. Note that for a massless field the expressions for the boundary-induced contributions in the expectation values are reduced to

$$\begin{aligned}\langle j^0 \rangle^{(b)} &= \frac{2eT}{\phi_0 a} \sum_j \sum_{n=0}^{\infty} \frac{I_{\beta_j+\epsilon_j}^2(zr/a) - I_{\beta_j}^2(zr/a)}{I_{\beta_j+\epsilon_j}^2(z) + I_{\beta_j}^2(z)}, \\ \langle j^2 \rangle^{(b)} &= \frac{2eT}{\phi_0} \sum_j \sum_{n=0}^{\infty} \sum_{\chi=\pm 1} \frac{\chi I_{\alpha_j-\chi\epsilon_j/2}(z) K_{\alpha_j-\chi\epsilon_j/2}(z)}{I_{\beta_j}^2(z) + I_{\beta_j+\epsilon_j}^2(z)} U_{2,\beta_j}^I(zr/a),\end{aligned}\quad (5.19)$$

where $z = (2n + 1)\pi aT$.

Now we turn to the zero temperature limit for the I-region. In the case of zero chemical potential that limit is directly obtained from (5.18) (or from (5.15) with $u_n = u_{n0}$) by the replacement (4.16) and we get the VEVs given by (3.7) in the region $r < a$. For $\mu \neq 0$, as a starting point it is convenient to use the representation (5.1). For the chemical potential in the range $\mu^2 < \gamma_{j,1}^{(\lambda)2}/a^2 + m^2$ the relation (4.17) takes place and the zero temperature expectation values coincide with the corresponding VEVs. In the case $\mu^2 > \gamma_{j,1}^{(\lambda)2}/a^2 + m^2$ one has $\lim_{T \rightarrow 0} [e^{\beta(E - \lambda\mu)} + 1] = 1$ for the modes with $E < \lambda\mu$ and $\lim_{T \rightarrow 0} [e^{\beta(E - \lambda\mu)} + 1] = 2$ for $E = \lambda\mu$. For the zero temperature limit of the expectation values from (5.1) we get

$$\langle j^\nu \rangle_{T=0} = \langle j^\nu \rangle_{\text{vac}} + \frac{\lambda e}{2\phi_0 a} \sum_j \sum_{l=1}^{l_m}' T_{\beta_j}^{(\lambda)}(\gamma_{j,l}^{(\lambda)}) g^{(\nu)}(\gamma_{j,l}^{(\lambda)}/a), \quad (5.20)$$

where λ and l_m are defined by $\mu = \lambda|\mu|$ and

$$\gamma_{j,l_m}^{(\lambda)} \leq a\gamma_F < \gamma_{j,l_m+1}^{(\lambda)}. \quad (5.21)$$

The prime on the summation over l means that in case of $\gamma_{j,l_m}^{(\lambda)} = a\gamma_F$ the term with $l = l_m$ must be taken with an additional factor 1/2. The last term in (5.20) comes from particles for $\mu > 0$ and antiparticles for $\mu < 0$. The zero temperature limit of the expectation values in the geometry without boundary is given by (4.19). In Appendix B we show that the same result (5.20) is obtained from the representation (5.15).

The MIT bag boundary condition (2.8) provides zero normal fermionic current on the boundary. The same is done by the boundary condition that differs from (2.8) by the sign of the term involving the normal to the boundary (see, e.g., [51]). We can combine both the conditions in

$$(1 + \eta i n_\mu \gamma^\mu) \psi(x) = 0, \quad r = a, \quad (5.22)$$

introducing the parameter $\eta = \pm 1$. It can be shown that the results for the boundary condition with $\eta = -1$ are obtained from the corresponding formulas for the condition (2.8) ($\eta = +1$) by the replacement $\delta^{(J)} \rightarrow -\delta^{(J)}$ in the definitions (2.15), (3.8), and (5.9). Equivalently, we can generalize the expressions for the edge induced expectation values in the case of the condition (5.22) by making the replacement $\delta^{(J)} \rightarrow \eta \delta^{(J)}$. The corresponding problem is specified by the set of parameters (s, μ, η) . From the definitions (3.8) and (4.9) it is seen that

$$\bar{F}_{\beta_j}(u_n a)|_{(s, \mu, \eta)} = [\bar{F}_{\beta_j}(u_n a)|_{(-s, -\mu, -\eta)}]^*. \quad (5.23)$$

Now, from (4.10) and (5.15) we get the following relations between the edge induced expectation values in two different problems with the sets (s, μ, η) and $(-s, -\mu, -\eta)$:

$$\langle j^\nu \rangle_{(s, \mu, \eta)}^{(b)} = (-1)^{1-\nu/2} \langle j^\nu \rangle_{(-s, -\mu, -\eta)}^{(b)}, \quad (5.24)$$

for $\nu = 0, 2$. Hence, the expectation values for the condition (5.22) with $\eta = -1$ are obtained from those in the case $\eta = +1$ (given above) by the replacements $s \rightarrow -s$ and $\mu \rightarrow -\mu$. In a similar way, from the formulas in Section 3 it can be seen that

$$\langle j^\nu \rangle_{(s, \mu)}^{(0)} = (-1)^{1-\nu/2} \langle j^\nu \rangle_{(-s, -\mu)}^{(0)}. \quad (5.25)$$

This shows that the relation (5.24) takes place for the total expectation values $\langle j^\nu \rangle_{(s, \mu, \eta)}$ as well.

The mode functions used above in the investigations of the charge and current densities in the E- and I-regions are periodic functions of the angular coordinate ϕ with the period ϕ_0 . We could impose more general periodicity condition with a nontrivial phase, given by $\psi(t, r, \phi + \phi_0) = e^{2\pi i \zeta} \psi(t, r, \phi)$, where ζ is

a constant. It can be checked that the fermionic modes in this case are obtained from those discussed above by the shift $j \rightarrow j + \varsigma$. The corresponding expressions for the expectation values of the charge and current densities are given by the formulas given above making the replacement $\alpha \rightarrow eA/q + \varsigma$. This shows that the phase ς can be interpreted in terms of the Aharonov-Bohm type vector potential and vice versa.

6 Asymptotic and numerical analysis

In this section we investigate the asymptotics for the boundary-induced expectation values of the charge and current densities corresponding to the limiting values of radial coordinate r , temperature T and parameters a, α_0 .

6.1 Radial asymptotics

Firstly, we consider the expectation values in the E-region at large distances from the circular boundary by fixing the location of the boundary, the chemical potential and the mass. By taking into account that for large $|z|$ one has $K_\beta(z) \sim \sqrt{\pi/2ze^{-z}}$, from (4.10) we find

$$\langle j^\nu \rangle^{(b)} \approx \frac{2\pi eT}{r^2 \phi_0} \sum_j \sum_{n=0}^{\infty} \operatorname{Re} \left[\frac{\bar{I}_{\beta_j}(u_n a)}{\bar{K}_{\beta_j}(u_n a)} \left(\frac{smr}{u_n} \right)^{1-\nu/2} e^{-2ru_n} \right]. \quad (6.1)$$

For temperatures $T \gtrsim m, |\mu|$ the series over n is dominated by the first term and one gets $\langle j^\nu \rangle^{(b)} \propto e^{-2ru_0}$. In the case $\mu = 0$ the large distance asymptotic is further simplified with the current density

$$\langle j^2 \rangle^{(b)} \approx \frac{2\pi eT}{\phi_0 r^2} \sum_j \frac{W_j^{(E)}(z) e^{-2zr/a}}{K_{\beta_j+\epsilon_j}^2(z) + K_{\beta_j}^2(z) + 2sm_a K_{\beta_j}(z) K_{\beta_j+\epsilon_j}(z)/z}, \quad (6.2)$$

where $z = a\sqrt{\pi^2 T^2 + m^2}$. The charge density is expressed as

$$\langle j^0 \rangle^{(b)} \approx \frac{sm \langle j_\phi \rangle^{(b)}}{\sqrt{\pi^2 T^2 + m^2}}. \quad (6.3)$$

For a massless field the leading term for the charge density in (6.3) vanishes and keeping the next term in the expansion one finds

$$\langle j^0 \rangle^{(b)} \approx \frac{4e}{\phi_0^2 T a r^2} \sum_j \frac{(j + \alpha_0) e^{-2\pi T r}}{K_{\beta_j+\epsilon_j}^2(\pi T a) + K_{\beta_j}^2(\pi T a)}. \quad (6.4)$$

It is of interest to compare the large distance asymptotics with those for the expectation value $\langle j^\nu \rangle^{(0)}$ in the boundary-free conical space. The leading term for the charge density $\langle j^0 \rangle^{(0)}$ coincides with the expectation value $\langle j^0 \rangle^{(M)}$ in the Minkowski spacetime with $\alpha_0 = 0$, given by (3.16). The latter does not depend on the radial coordinate. The topological contribution induced by a boundary-free conical geometry and magnetic flux is described by the difference $\langle j^\nu \rangle_t^{(0)} = \langle j^\nu \rangle^{(0)} - \langle j^\nu \rangle^{(M)}$, with $\langle j^2 \rangle^{(M)} = 0$. For $\phi_0 > \pi$ the topological part $\langle j^\nu \rangle_t^{(0)}$ is suppressed by the factor e^{-2ru_0} . In the case $\phi_0 < \pi$ the suppression of the expectation value $\langle j^\nu \rangle_t^{(0)}$ is weaker, by the factor $e^{-2ru_0 \sin(\phi_0/2)}$. For a massive field the asymptotics of the VEVs in a boundary-free conical space are described by

$$\begin{aligned} \langle j^\nu \rangle_{\text{vac}}^{(0)} &\propto e^{-2mr}, \quad mr \gg 1, \quad \phi_0 > \pi, \\ \langle j^\nu \rangle_{\text{vac}}^{(0)} &\propto e^{-2mr \sin(\phi_0/2)}, \quad mr \gg 1, \quad \phi_0 < \pi. \end{aligned} \quad (6.5)$$

For a massless field the charge density vanishes, $\langle j^0 \rangle_{\text{vac}}^{(0)} = 0$, and the decay of the current density follows a power-law, like $\langle j^2 \rangle_{\text{vac}}^{(0)} \propto 1/r^2$. At large distances the boundary-induced contributions in the VEVs behave like $\langle j^0 \rangle_{\text{vac}}^{(b)}, \langle j_\phi \rangle_{\text{vac}}^{(b)} \propto e^{-2mr}/r^{3/2}$, $mr \gg 1$, for a massive field and as $\langle j^0 \rangle_{\text{vac}}^{(b)} \propto 1/r^{2\rho+2}$ in the case of a massless field. Here, we have defined

$$\rho = q (1/2 - |\alpha_0|). \quad (6.6)$$

In the case of a massless field for the boundary-induced VEV of the current density one has $\langle j_\phi \rangle_{\text{vac}}^{(b)} \propto 1/r^{2\rho+3}$ for $\rho > 1/2$ and $\langle j_\phi \rangle_{\text{vac}}^{(b)} \propto 1/r^{4\rho+2}$ for $\rho < 1/2$.

In Figure 2 we have plotted the radial dependence of the boundary-induced contributions in the charge and current densities in the E-region for $m = \mu = 0$ and for fixed temperature corresponding to $Ta = 0.5$. The full and dashed curves correspond to $\alpha_0 = 0.2$ and $\alpha_0 = 0.4$, respectively, and the numbers near the curves present the values of the parameter q . An important feature for the charge and current densities is their finiteness in the limit $r \rightarrow a$. This is in contrast to the behavior of the fermion condensate that diverges on the edge (see [45]).

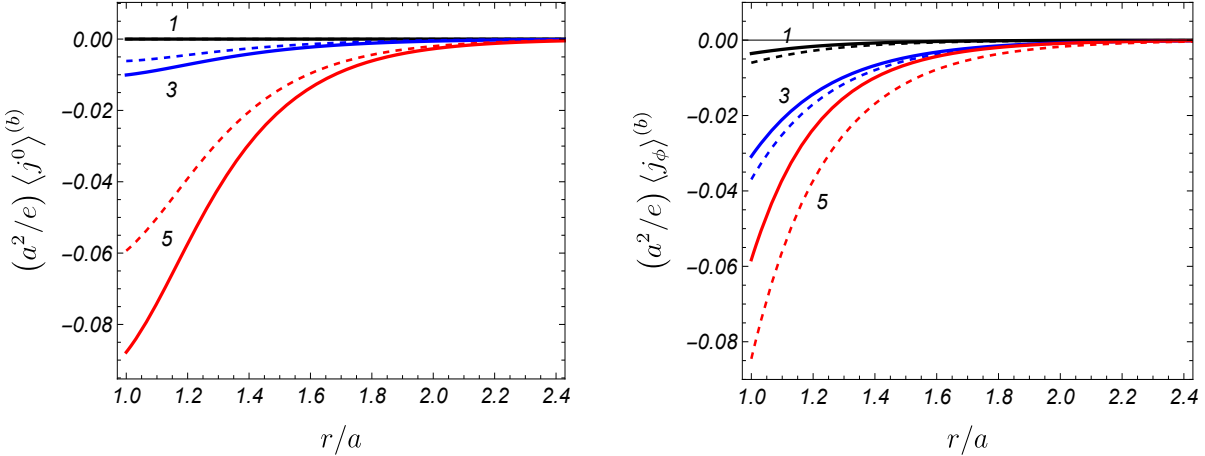


Figure 2: Expectation values of the charge (left panel) and current (right panel) densities in the E-region for a massless field with zero chemical potential as functions of the radial coordinate. The graphs are plotted for $Ta = 0.5$ and the full/dashed curves correspond to $\alpha_0 = 0.2/\alpha_0 = 0.4$. The numbers near the curves are the values of q .

The difference in the near-boundary behavior of the fermion condensate from one side and the charge and current densities from the other side can also be understood by general arguments of quantum field theory in external fields. In quantum field theory with boundaries the divergences in the expectation values of local physical observables, bilinear in the field operator, are divided into bulk and boundary divergences. For a given quantum field in an external gauge field $A_\mu(x)$, the bulk divergences are uniquely determined by the local geometrical characteristics of the spacetime, constructed from the Riemann tensor, and by the gauge field strength tensor $F_{\mu\nu}$. For smooth boundaries, the boundary divergences are specified by the extrinsic curvature tensor of the boundary [52, 53] (see also [10, 11] for discussions in the context of the Casimir effect). An important point is that the boundary divergences are entirely due to the vacuum parts in the expectation values. In the problem under consideration the field tensor $F_{\mu\nu}$ is zero and the background geometry is flat except the point corresponding to the cone apex $r = 0$ in the I-region. Consequently, the renormalization of the expectation values of local observables for $r \neq 0$ and $r \neq a$ is realized by the subtraction of the corresponding quantities for the boundary-free Minkowski spacetime in the absence of the gauge field. The vacuum contributions in the expectation values of the charge and current densities are odd functions of the parameter α , determined by magnetic flux in accordance with (2.12). From here it follows that in the problem with zero gauge field ($A_\mu = 0$ and

$\alpha = 0$) the renormalized charge and current densities become zero everywhere including the points on the boundary. Now, when we add an external constant gauge field, the bulk and boundary geometries are not changed and the field tensor remains equal to zero. Thus, the divergences in the problems without and with constant gauge fields are the same. In particular, the turning on of the constant gauge field does not add boundary divergences in the expectation values of the charge and current densities. Note that the given argument does not work for the fermion condensate. The latter is an even function of α and it does vanish for $\alpha = 0$. The vacuum fermion condensate diverges on the boundary and the diverging contribution does not depend on the parameter α .

For a massless field with zero chemical potential the charge density in the boundary-free geometry vanishes, $\langle j^0 \rangle^{(0)} = 0$, and the boundary induced contribution in the charge density plotted in Figure 2 coincides with the total charge density $\langle j^0 \rangle$. That is not the case for the current density. For $m = \mu = 0$ the current density in a conical space without boundary is expressed as [34]

$$\begin{aligned} \langle j_\phi \rangle^{(0)} = & -\frac{4eT^3r}{\pi} \sum_{n=0}^{\infty}' (-1)^n \left\{ \sum_{l=1}^{[q/2]} \frac{(-1)^l \sin(\pi l/q) \sin(2\pi l\alpha_0)}{\left[n^2 + (2Tr \sin(\pi l/q))^2 \right]^{\frac{3}{2}}} \right. \\ & \left. - \frac{q}{\pi} \int_0^\infty dy \frac{f(q, \alpha_0, y) \cosh y}{\cosh(2qy) - \cos(q\pi)} \frac{1}{[n^2 + (2Tr \cosh y)^2]^{\frac{3}{2}}} \right\}, \end{aligned} \quad (6.7)$$

where the function $f(q, \alpha_0, y)$ is defined by Eq. (3.5) and the prime on the sum over n means that the term $n = 0$ is taken with the coefficient $1/2$ (for the prime on the sum over l see (3.4)). That term corresponds to the vacuum current density $\langle j_\phi \rangle_{\text{vac}}^{(0)}$ and the remaining part presents the thermal contribution. In the massless case the vacuum current density behaves like $\langle j_\phi \rangle_{\text{vac}}^{(0)} \propto 1/r^2$. For comparison with the contributions induced by the boundary, Figure 3 shows the radial dependence of the thermal contribution to the current density, $\langle j_\phi \rangle_T^{(0)}$, for a massless field with zero chemical potential in the boundary-free geometry (full curves) for $Ta = 0.5$ and $\alpha_0 = 0.2$. The numbers near the curves present the corresponding values of q . The dashed curves describe the radial dependence of the vacuum current density, $\langle j_\phi \rangle_{\text{vac}}$, in the same geometry for $\alpha_0 = 0.2$. Although the problem corresponding to Figure 3 does not contain the parameter a , the quantities on the horizontal and vertical axes correspond to the radial distance and the current density measured in units of a and e/a^2 , respectively. This choice of the measurement units makes it easier to compare with data in figures for the geometry with the boundary.

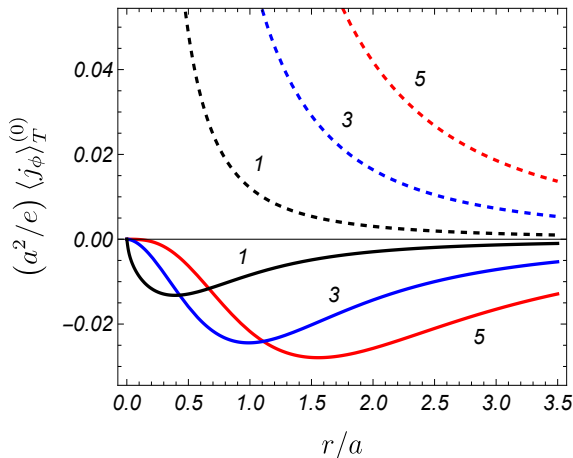


Figure 3: Vacuum (dashed curves) and thermal (full curves) current densities for a massless field with zero chemical potential in the boundary-free geometry. For the parameters we have taken $Ta = 0.5$, $\alpha_0 = 0.2$, and the numbers near the curves are the values of q .

Now we consider the asymptotic of the boundary-induced expectation values (5.15) in the I-region for points near the cone apex. In the limit of small values of r the series over j is dominated by the contribution of the mode with $j = -\text{sgn}(\alpha_0)/2$ and, by using the small argument asymptotic for the function $I_\beta(z)$, the leading order terms read

$$\begin{aligned}\langle j^0 \rangle^{(b)} &\approx \frac{2\text{sgn}(\alpha_0) eT (r/2)^{2\rho-1}}{\phi_0 \Gamma^2(\rho + 1/2)} \sum_{n=0}^{\infty} \text{Re} \left\{ u_n^{2\rho-1} \right. \\ &\quad \left. \times \frac{\bar{K}_{\beta_j}(u_n a)}{\bar{I}_{\beta_j}(u_n a)} [\pi(2n+1)T - i\mu + i\text{sgn}(\alpha_0)sm] \right\}, \\ \langle j^2 \rangle^{(b)} &\approx \frac{-4eT (r/2)^{2\rho-1}}{\phi_0 (2\rho + 1) \Gamma^2(\rho + 1/2)} \sum_{n=0}^{\infty} \text{Re} \left[\frac{\bar{K}_{\beta_j}(u_n a)}{\bar{I}_{\beta_j}(u_n a)} u_n^{2\rho+1} \right].\end{aligned}\quad (6.8)$$

As seen, the physical component $\langle j_\phi \rangle^{(b)}$ of the boundary-induced current density vanishes on the cone apex. According to (6.8), the boundary-induced charge density vanishes on the cone apex for $\rho > 1/2$ and diverges for $\rho < 1/2$. For $\rho = 1/2$ it takes a finite nonzero limiting value.

In the limit $r \rightarrow 0$, the VEVs in a boundary-free conical space behave as $\langle j^\nu \rangle_{\text{vac}}^{(0)} \propto 1/r^{1+\nu}$ (see (3.4)). In the case of a massless field the corresponding charge density vanishes. The near-apex asymptotic of the thermal part of the expectation value in the boundary-free geometry, $\langle j^\nu \rangle_T^{(0)} = \langle j^\nu \rangle^{(0)} - \langle j^\nu \rangle_{\text{vac}}^{(0)}$, is given by $\langle j^\nu \rangle_T^{(0)} \propto r^{2\rho-1}$ for $\rho < 1/2$. For the values of the parameters in the region $\rho > 1/2$ the thermal expectation value $\langle j^\nu \rangle_T^{(0)}$ tends to a finite nonzero value in the limit $r \rightarrow 0$. We see that near the apex the expectation values of the charge and current densities are dominated by the vacuum parts independent of a . The radial dependence of the boundary-induced charge and current densities in the I-region is plotted in Figure 4 for the same values of the parameters as in Figure 2. As follows from the asymptotic analysis, at the cone apex the boundary-induced expectation value of the current density $\langle j_\phi \rangle^{(b)}$ always vanishes, whereas the boundary-induced expectation value of the charge density diverges in case of $2|\alpha_0| > 1 - 1/q$ and vanishes for $2|\alpha_0| < 1 - 1/q$. In the special case $2|\alpha_0| = 1 - 1/q$ the charge density tends to a finite nonzero value in the limit $r \rightarrow 0$. On the left panel of Figure 4 that case corresponds to the dashed curve for $q = 5$. In addition, for large values of Tr the boundary-induced expectation values are suppressed by the factor $e^{-2\pi T(r-a)}$.

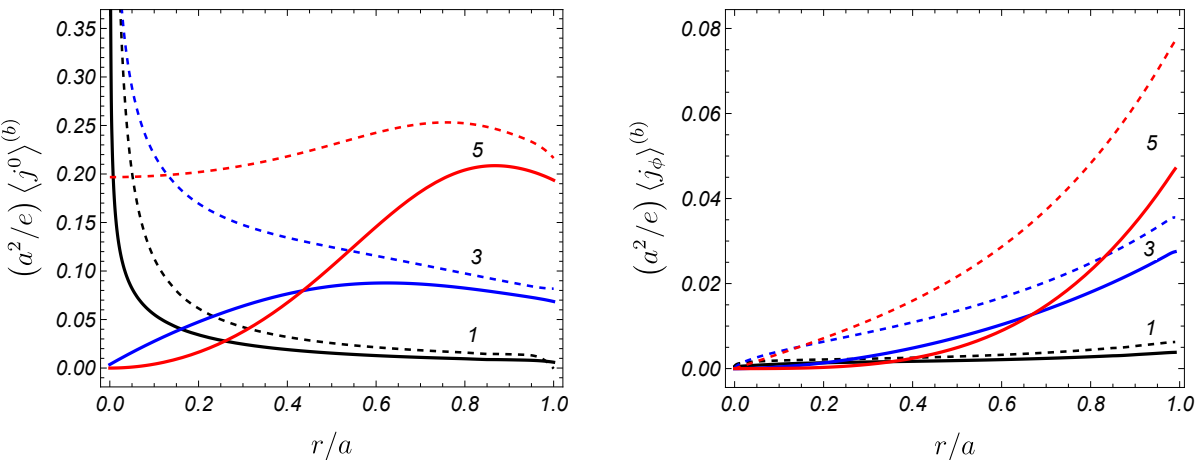


Figure 4: The same as in Figure 2 for the I-region.

It is also of interest to consider the behavior of the boundary-induced expectation values for small values of the radius a and for fixed r , assuming that $Ta, ma \ll 1$. By using the asymptotic expressions for the modified Bessel functions for small values of the argument, from (4.10) one can see that

$\langle j^0 \rangle^{(b)}, \langle j_\phi \rangle^{(b)} \propto a^{2\rho}$ and for $|\alpha_0| < 1/2$ the boundary-induced contributions tend to zero in the limit $a \rightarrow 0$. The expectation values of the charge and current densities in the limit $|\alpha_0| \rightarrow 1/2$ are discussed in the next subsection. This limit corresponds to a half-integer magnetic flux in units of the flux quantum.

6.2 Charge and current densities for half-integer fluxes

The charge and current densities, in general, are discontinuous at half-integer values of the parameter α . By taking into account that the expectation values are periodic functions of α with the period equal to 1, the discontinuity at $\alpha = 1/2$ can be expressed as

$$\langle j^\nu \rangle|_{\alpha=1/2-0}^{\alpha=1/2+0} = \langle j^\nu \rangle|_{\alpha_0=1/2-0}^{\alpha_0=-1/2+0} \equiv \langle j^\nu \rangle|_{\alpha_0=1/2}^{\alpha_0=-1/2}. \quad (6.9)$$

Here and below, $\alpha_0 = \pm 1/2$ is understood in the sense $\alpha_0 \rightarrow \pm (1/2 - 0)$.

First we consider the expectation values in the boundary-free conical geometry. By using the expressions $\langle j^\nu \rangle^{(0)}$ from [34] we get

$$\langle j^\nu \rangle^{(0)}|_{\alpha_0=1/2}^{\alpha_0=-1/2} = -\frac{2^{7/2} em^2 s}{\pi^{3/2} \phi_0} (2ms)^{\frac{\nu}{2}} \sum_{n=0}^{\infty}' (-1)^n \cosh(n\mu/T) \int_0^\infty dy h_{\frac{1+\nu}{2}}(c_n(y)) \cosh y, \quad (6.10)$$

with the functions $h_\beta(x) = x^{-\beta} K_\beta(x)$ and $c_n(y) = m\sqrt{n^2/T^2 + 4r^2 \cosh^2 y}$. Here, the prime on the summation sign means that the term $n = 0$ is taken with an additional coefficient 1/2. Note that the current density $\langle j^2 \rangle^{(0)}$ is an even function of the chemical potential (and, hence, an odd function of α) and the corresponding limiting values are expressed as $\langle j^2 \rangle^{(0)}|_{\alpha_0=\pm 1/2} = \mp \langle j^2 \rangle^{(0)}|_{\alpha_0=1/2}^{\alpha_0=-1/2}/2$. Introducing a new integration variable $w = c_n(y)$, the integral in (6.10) is evaluated by using the formula from [48] with the result

$$\int_0^\infty dy \cosh y h_{\frac{1+\nu}{2}}(c_n(y)) = \frac{\sqrt{\pi/2}}{2mr} h_{\frac{\nu}{2}}(m\sqrt{n^2/T^2 + 4r^2}). \quad (6.11)$$

This gives

$$\langle j^\nu \rangle^{(0)}|_{\alpha_0=1/2}^{\alpha_0=-1/2} = -\frac{4esm}{\pi\phi_0 r} (2ms)^{\frac{\nu}{2}} \sum_{n=0}^{\infty}' (-1)^n \cosh(n\mu/T) h_{\frac{\nu}{2}}(m\sqrt{n^2/T^2 + 4r^2}). \quad (6.12)$$

In particular, for $\mu = 0$ from here it follows that

$$\langle j^\nu \rangle^{(0)}|_{\alpha_0=\pm 1/2} = \pm \frac{2esm}{\pi\phi_0 r} (2ms)^{\frac{\nu}{2}} \sum_{n=0}^{\infty}' (-1)^n h_{\frac{\nu}{2}}(m\sqrt{n^2/T^2 + 4r^2}). \quad (6.13)$$

Now we turn to the boundary-induced contributions. By using the definitions of β_j and ϵ_j , it can be seen that for a function $f(x, y)$ one has

$$\sum_j f(\beta_j, \beta_j + \epsilon_j)|_{\alpha_0=\pm 1/2} = \sum_{l=1}^{\infty} \sum_{\chi=\pm 1} f(ql - \chi/2, ql + \chi/2) + f(\pm 1/2, \mp 1/2), \quad (6.14)$$

where the last term comes from the $j = \mp 1/2$ mode for $\alpha_0 = \pm 1/2$. From here it follows that the discontinuity at $\alpha = 1/2$ is determined by

$$\sum_j f(\beta_j, \beta_j + \epsilon_j)|_{\alpha_0=1/2}^{\alpha_0=-1/2} = f(-1/2, 1/2) - f(1/2, -1/2), \quad (6.15)$$

and it comes from the mode $j = \mp 1/2$ for $\alpha_0 = \pm 1/2$.

Taking the expressions of the function $f(\beta_j, \beta_j + \epsilon_j)$ from (4.10), for the expectation values of the charge and current densities in the E-region we find

$$\langle j^\nu \rangle^{(b)}|_{\alpha_0=1/2}^{\alpha_0=-1/2} = (sm)^{1-\frac{\nu}{2}} \frac{4Te}{\phi_0} \sum_{n=0}^{\infty} \operatorname{Re} \left[\left(\frac{u_n}{r} \right)^{\frac{\nu}{2}} [I_{-1/2}(u_n a) - I_{1/2}(u_n a)] \frac{K_{1/2}^2(u_n r)}{K_{1/2}(u_n a)} \right], \quad (6.16)$$

with $\nu = 0, 2$. The combination of the modified Bessel functions is simplified to $e^{-2u_n r}/(u_n r)$ and one gets

$$\langle j^\nu \rangle^{(b)}|_{\alpha_0=1/2}^{\alpha_0=-1/2} = \frac{2Te}{\phi_0 r^{1+\frac{\nu}{2}}} \sum_{n=-\infty}^{+\infty} \left(\frac{sm}{u_n} \right)^{1-\frac{\nu}{2}} e^{-2u_n r}. \quad (6.17)$$

Note that the right-hand side does not depend on the radius a of the boundary. In the special case of zero chemical potential, $\mu = 0$, the expectation values are odd functions of α_0 and from here we get

$$\langle j^\nu \rangle^{(b)}|_{\alpha_0=\pm 1/2} = \mp \frac{Te}{\phi_0 r^{1+\frac{\nu}{2}}} \sum_{n=-\infty}^{+\infty} \left(\frac{sm}{u_{0n}} \right)^{1-\frac{\nu}{2}} e^{-2u_{0n} r}. \quad (6.18)$$

In particular, for a massless field the charge density is continuous.

Alternative representations for the discontinuities in the E-region are obtained from (6.17) by applying the formula [54, 55]

$$\sum_{n=-\infty}^{+\infty} w_n^{2\beta-1} h_{\beta-1/2}(2rw_n) = \frac{m^{2\beta}}{\sqrt{2\pi}T} \sum_{n=-\infty}^{+\infty} \cos(n\alpha) h_\beta(m\sqrt{4r^2 + n^2/T^2}), \quad (6.19)$$

with $w_n = \sqrt{(2\pi n + \alpha)^2 T^2 + m^2}$. For $\alpha = \pi - i\mu/T$ the series in the left-hand side of (6.19) coincides with the series in (6.17) for the charge density ($\nu = 0$) in the case $\beta = 0$ and for the current density ($\nu = 2$) in the case $\beta = 1$. Applying the formula (6.19) in these special cases, from (6.17) one gets

$$\langle j^\nu \rangle^{(b)}|_{\alpha_0=1/2}^{\alpha_0=-1/2} = \frac{4esm}{\pi\phi_0 r} (2ms)^{\frac{\nu}{2}} \sum_{n=0}^{\infty}' (-1)^n \cosh(n\mu/T) h_{\frac{\nu}{2}}(m\sqrt{n^2/T^2 + 4r^2}). \quad (6.20)$$

Combining this expression with the corresponding result (6.12) for the boundary-free geometry we see that in the E-region the total expectation value (3.1) is continuous at half-integer values of the parameter α : $\langle j^\nu \rangle|_{\alpha_0=1/2}^{\alpha_0=-1/2} = 0$. The boundary conditions used above for the confinement of the field separate the field fluctuations in the E-region from the cone apex and magnetic flux. All the fermionic modes in that region are regular and the total expectation values are continuous functions of the parameter α .

Figure 5 displays the boundary-induced expectation values of the charge and current densities for a massless field with zero chemical potential in the E-region versus the parameter α_0 for fixed values of $r/a = 1.5$ and $Ta = 0.5$. The numbers near the curves correspond to the values $q = 1, 3, 4, 5$ for the parameter describing the planar angle deficit. For the considered example one has $\langle j^0 \rangle^{(0)} = 0$ and both the total and boundary induced charge densities are continuous at half integer values of the parameter α ($\langle j^0 \rangle|_{\alpha_0=\pm 1/2} = \langle j^0 \rangle|_{\alpha_0=\pm 1/2}^{(b)} = 0$ for $\mu = 0$). For the current density the part independent of a is given by (6.7) and it is discontinuous at half integer values of α . This discontinuity cancels the discontinuity of the boundary-induced expectation value, depicted on the right panel of Figure 5, and the total current density in the E-region is continuous, in accordance with the asymptotic analysis given above.

In the way similar to that for the E-region, the discontinuities of the boundary induced expectation values in the I-region are expressed as

$$\begin{aligned} \langle j^0 \rangle^{(b)}|_{\alpha_0=1/2}^{\alpha_0=-1/2} &= \frac{8eT}{\phi_0 r} \sum_{n=0}^{\infty} \operatorname{Re} \left[\frac{sm \cosh(2u_n r) - (u_n + sm) e^{2u_n a}}{u_n \left(\frac{u_n + sm}{u_n - sm} e^{4u_n a} + 1 \right)} \right], \\ \langle j^2 \rangle^{(b)}|_{\alpha_0=1/2}^{\alpha_0=-1/2} &= -\frac{8eT}{\phi_0 r^2} \sum_{n=0}^{\infty} \operatorname{Re} \left[\frac{\sinh(2u_n r)}{\frac{u_n + sm}{u_n - sm} e^{4u_n a} + 1} \right]. \end{aligned} \quad (6.21)$$

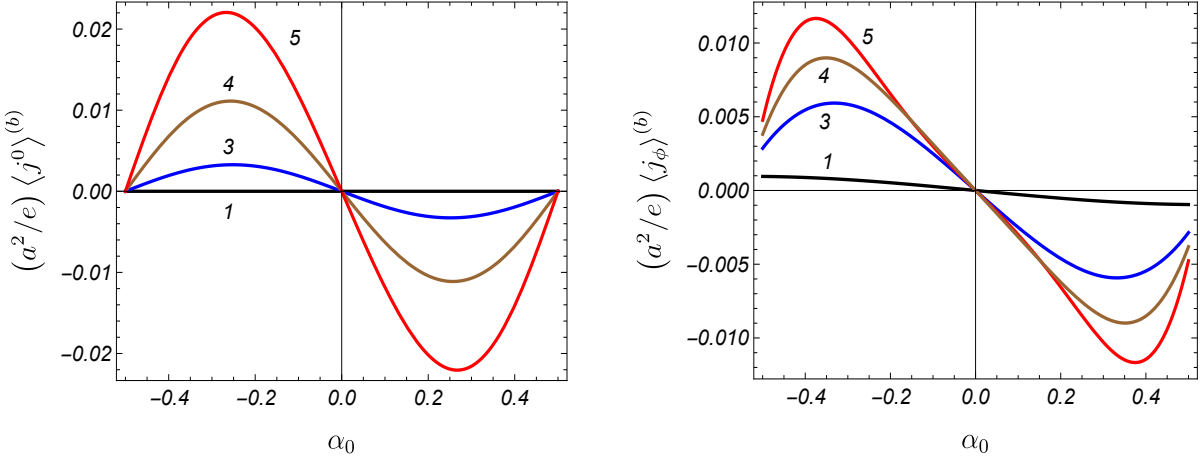


Figure 5: Expectation values of the charge (left panel) and current (right panel) densities in the E-region for a massless field with a zero chemical potential versus the parameter α_0 . The graphs are plotted for $r/a = 1.5$, $Ta = 0.5$ and the numbers near the curves correspond to the values of q .

For $\mu = 0$ from here we find

$$\begin{aligned} \langle j^0 \rangle^{(b)}|_{\alpha_0=\pm 1/2} &= \pm \frac{4eT}{\phi_0 r} \sum_{n=0}^{\infty} \frac{(u_{0n} + sm) e^{2u_{0n}a} - sm \cosh(2u_{0n}r)}{u_{0n} \left(\frac{u_{0n}+sm}{u_{0n}-sm} e^{4u_{0n}a} + 1 \right)}, \\ \langle j^2 \rangle^{(b)}|_{\alpha_0=\pm 1/2} &= \pm \frac{4eT}{\phi_0 r^2} \sum_{n=0}^{\infty} \frac{\sinh(2u_{0n}r)}{\frac{u_{0n}+sm}{u_{0n}-sm} e^{4u_{0n}a} + 1}. \end{aligned} \quad (6.22)$$

Unlike to the case of the E-region, the total expectation values in the I-region are discontinuous at half-integer values of α . By taking into account that the expectation value $\langle j^\nu \rangle^{(0)}|_{\alpha_0=1/2}^{\alpha_0=-1/2}$ is given by the right-hand side of (6.17) with the opposite sign, for the discontinuities in the I-region we get

$$\begin{aligned} \langle j^0 \rangle|_{\alpha_0=1/2}^{\alpha_0=-1/2} &= -\frac{4eT}{\phi_0 r} \sum_{n=0}^{\infty} \operatorname{Re} \left[\frac{sm \left(\frac{u_n+sm}{u_n-sm} e^{2u_n(a-r)} - e^{-2u_n(a-r)} \right) + 2(u_n + sm)}{u_n \left(\frac{u_n+sm}{u_n-sm} e^{2u_n a} + e^{-2u_n a} \right)} \right], \\ \langle j^2 \rangle|_{\alpha_0=1/2}^{\alpha_0=-1/2} &= -\frac{4eT}{\phi_0 r^2} \sum_{n=0}^{\infty} \operatorname{Re} \left[\frac{\frac{u_n+sm}{u_n-sm} e^{2u_n(a-r)} + e^{-2u_n(a-r)}}{\frac{u_n+sm}{u_n-sm} e^{2u_n a} + e^{-2u_n a}} \right]. \end{aligned} \quad (6.23)$$

In particular, it can be checked that for $r = a$ one has $\langle j^0 \rangle|_{\alpha_0=1/2}^{\alpha_0=-1/2} = r \langle j^2 \rangle|_{\alpha_0=1/2}^{\alpha_0=-1/2}$, in accordance with (5.3). The dependence of the boundary-induced charge and current densities in the I region on the parameter α_0 is presented in Figure 6 for $r/a = 0.5$. The values of the remaining parameters are the same as those for Figure 5. For the example presented in Figure 6 we have taken $m = \mu = 0$ and the charge density in the boundary-free geometry vanishes. Hence, the graphs on the left panel also present the total charge density. As explained above, both the boundary-free and boundary induced contributions are discontinuous at half-integer values of α .

6.3 Asymptotics and numerical analysis with respect to other parameters

In the high temperature limit, $T \gg m, |\mu|, 1/(r-a)$, the contributions of the $n = 0$ terms dominate in (4.10) and (5.15). In that limit the boundary-induced expectation values of the charge and current densities for a given r are suppressed by the factor $e^{-2\pi T(r-a)}$. The corresponding asymptotics for the parts independent of a have been discussed in [34]. For the topological part of the charge density in a

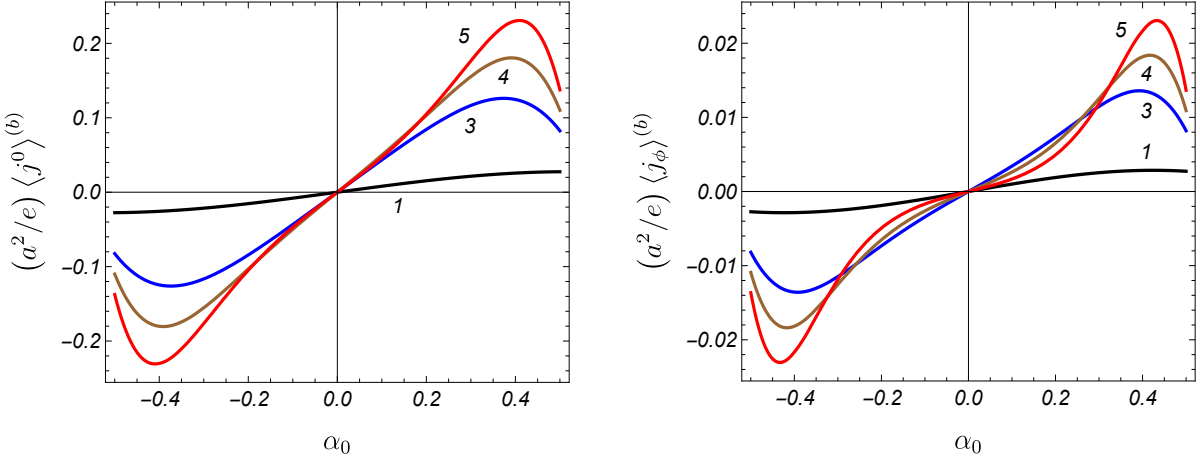


Figure 6: The same as in Figure 5 for the I-region. The expectation values are evaluated for $r/a = 0.5$ and for the same values of the remaining parameters as in Figure 5.

conical space without boundary one has $\langle j^0 \rangle_t^{(0)} \propto e^{-2\pi Tr \sin(\phi_0/2)}$ for $\phi_0 < \pi$. In the case $\phi_0 > \pi$ the decay is faster, like $\langle j^0 \rangle_t^{(0)} \propto e^{-2\pi Tr}$. As a consequence, at high temperatures and for points not too close to the boundary, the total charge density is dominated by the Minkowskian part which behaves like $\langle j^0 \rangle_M^{(0)} \approx e\mu T \ln 2/\pi$, provided that the chemical potential is nonzero. In the case of $\mu = 0$ the Minkowskian part vanishes. Similarly, for the current density independent of a one has $\langle j_\phi \rangle^{(0)} \propto e^{-2\pi Tr \sin(\phi_0/2)}$ for $\phi_0 < \pi$ and $\langle j_\phi \rangle^{(0)} \propto e^{-2\pi Tr}$ in the region $\phi_0 > \pi$. The zero temperature limit of the expectation values is analyzed in appendix B. As it has been shown, in the region $|\mu| > m$ for the chemical potential the expectation values differ from the respective vacuum counterparts. The corresponding asymptotic expressions are given by (4.19) for boundary-free geometry and by (4.18) and (5.20) for the boundary-induced contributions in the E- and I-regions, respectively. For a massless field with zero chemical potential, the Figure 7 displays the expectation values of the charge (left panel) and current (right panel) densities in the E-region versus the temperature. The graphs are plotted for $r/a = 1.5$ and for several values of the parameter q indicated next to the curves. The full and dashed curves correspond to $\alpha_0 = 0.2$ and $\alpha_0 = 0.4$, respectively. For $q = 1$ the dependence of the charge density on α_0 is weak and for that case the full and dashed curves nearly coincide with each other. In accordance with the asymptotic analysis given above, the expectation values are suppressed exponentially at high temperatures. The same dependence in the I-region is depicted in Figure 8 for the value of the radial coordinate corresponding to $r/a = 0.5$.

Now we turn to the dependence on the planar angle deficit. For the expectation values in the E-region it is displayed in Figure 9 for the parameters $r/a = 1.5$, $Ta = 0.5$ (full curves) and $Ta = 0.25$ (dashed curves). The numbers near the curves correspond to the values $\alpha_0 = 0.2, 0.4$ for the parameter describing the magnetic flux. The same dependence in the I-region for the radial coordinate corresponding to $r/a = 0.5$ is presented in Figure 10. Note that the behavior of the boundary-induced expectation values as functions of q essentially depends on the value of α_0 .

The numerical examples presented in the discussion above are given for massless fields with zero chemical potential. For those fields the expectation values do not depend on the parameter s . In Figure 11, as another numerical example, we display the dependence of the boundary-induced expectation values in the E-region on the mass for a field with zero chemical potential. The graphs are plotted for $r/a = 1.5$ and with the parameters describing the deficit angle and the magnetic flux having the values $q = 2.5$ and $\alpha_0 = 0.4$. The full (dashed) curves present the case $s = 1$ ($s = -1$) and the numbers near the curves indicate the values of Ta . The corresponding graphs for the I-region, evaluated at $r/a = 0.5$, are depicted in Figure 12. As seen from the graphs the dependence on the mass, in general, is not monotonic. For

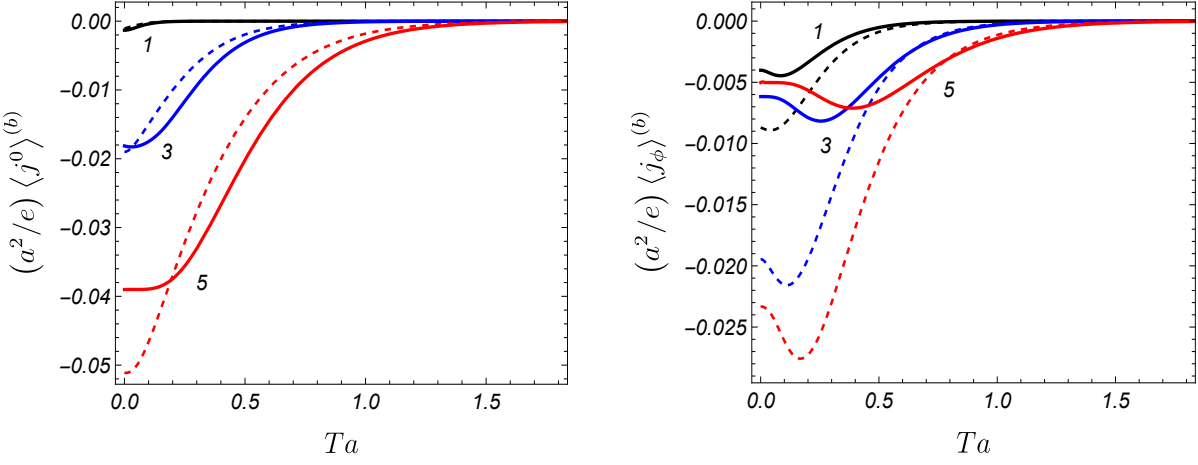


Figure 7: Expectation values of the charge (left panel) and current (right panel) densities in the E-region for a massless field with zero chemical potential versus the temperature. The graphs are plotted for $r/a = 1.5$ and the numbers near the curves correspond to the values of q . The full/dashed curves correspond to $\alpha_0 = 0.2/\alpha_0 = 0.4$.

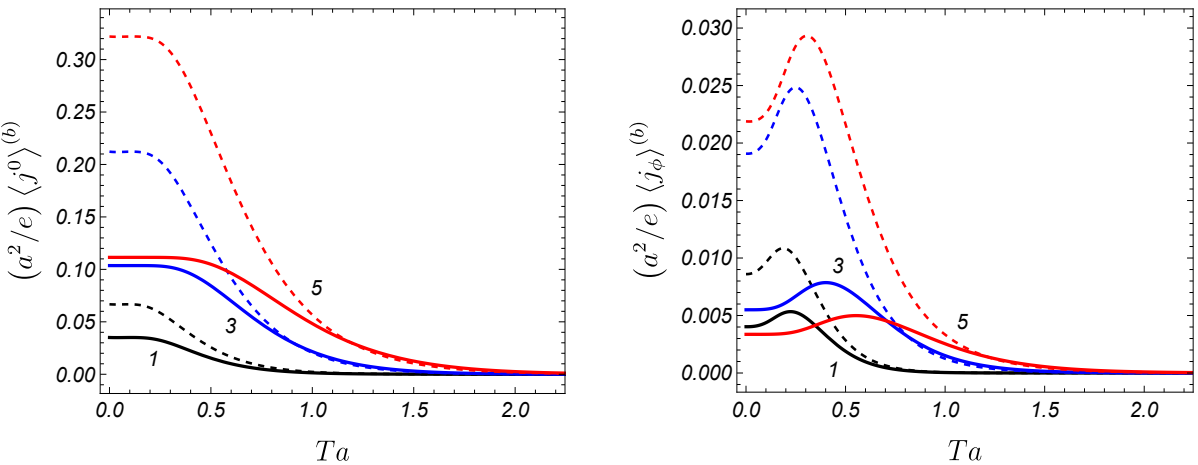


Figure 8: The same as in Figure 7 in the I-region for $r/a = 0.5$.

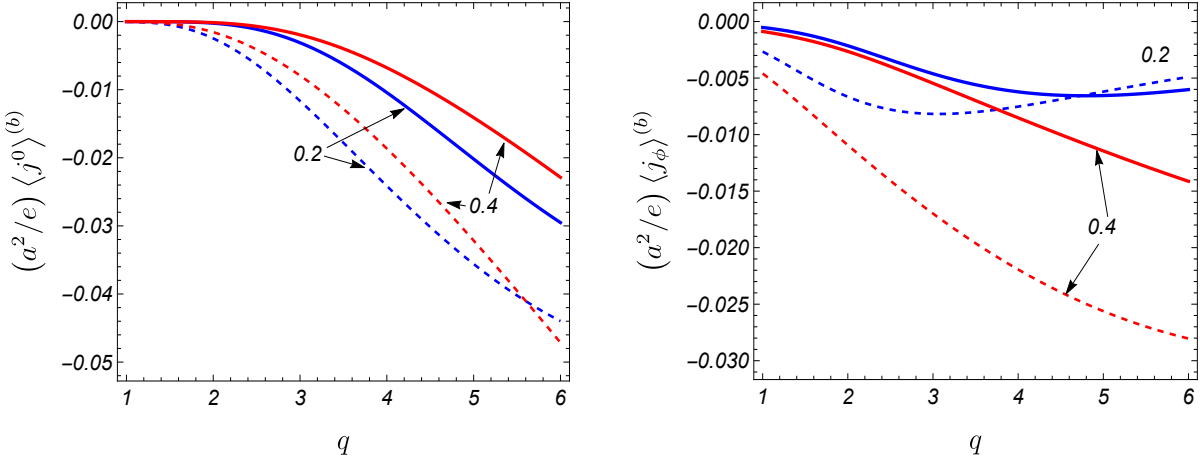


Figure 9: Expectation values of the charge (left panel) and current (right panel) densities for a massless field with zero chemical potential as functions of the parameter q . The graphs are plotted for $r/a = 1.5$, $Ta = 0.5$ (full curves), $Ta = 0.25$ (dashed curves) and the numbers near the curves are the corresponding values of α_0 .

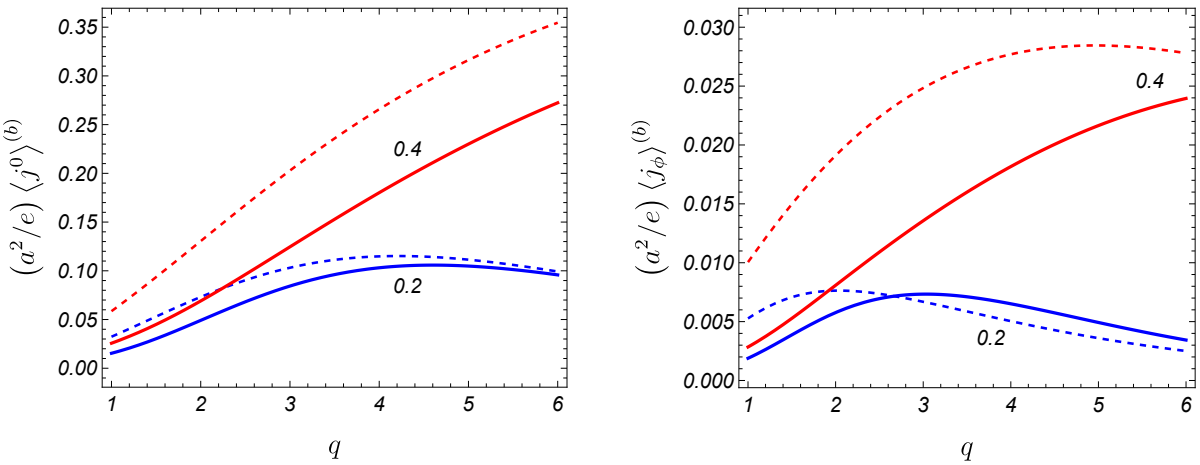


Figure 10: The same as in figure 9 for the I-region. For the radial coordinate the value $r/a = 0.5$ is taken.

fields with $s = -1$ the expectation values for massive fields can be essentially larger compared to the massless case.

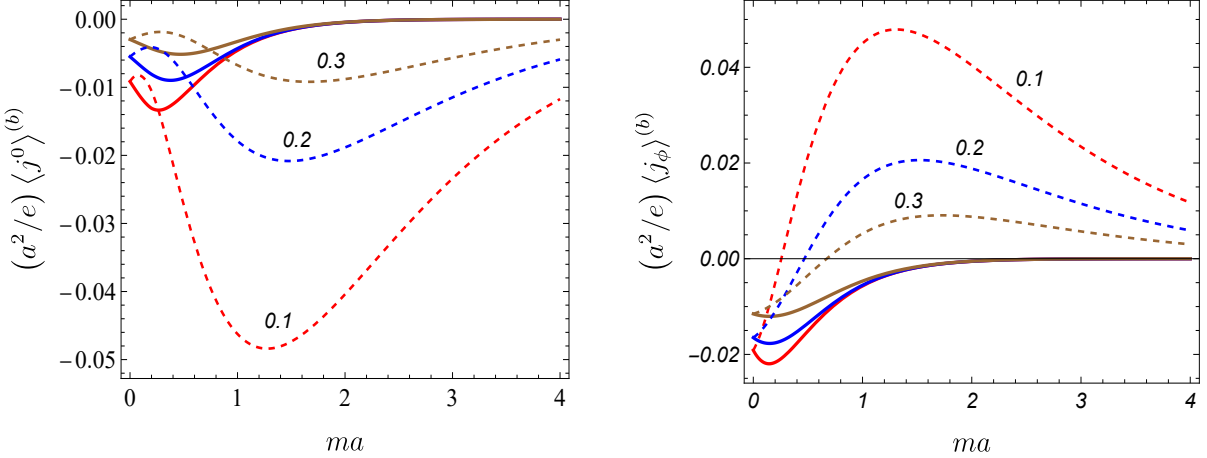


Figure 11: Boundary-induced expectation values of the charge (left panel) and current (right panel) densities in the E-region as functions of the field mass in the case of a zero chemical potential. The full and dashed curves correspond to $s = 1$ and $s = -1$, respectively. The numbers near the curves are the values of Ta and for remaining parameters we have taken $q = 2.5$, $\alpha_0 = 0.4$, and $r/a = 1.5$.

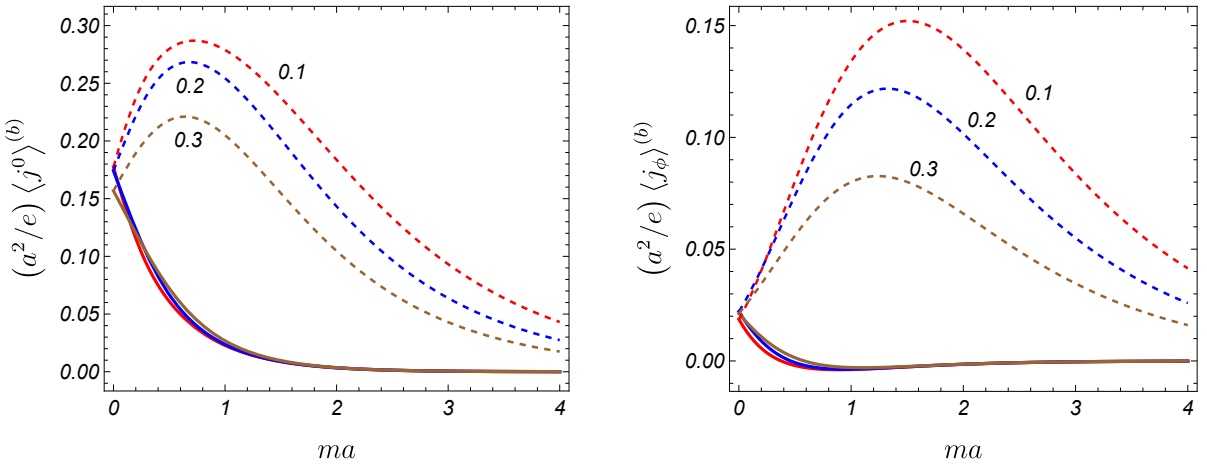


Figure 12: The same as in Figure 11 for the I-region with the value of the radial coordinate corresponding to $r/a = 0.5$.

7 Expectation values for the fields realizing two representations of the Clifford algebra

The inequivalent irreducible representations of the Clifford algebra in 3-dimensional spacetime described by (2.1) are realized by two sets of γ -matrices specified by $s = +1$ and $s = -1$ given as $\gamma_{(s)}^\mu = (\gamma^0, \gamma^1, \gamma_{(s)}^2)$ with $\gamma_{(s)}^2 = -is\gamma^0\gamma^1/r$ in the coordinates (t, r, ϕ) . Note that the matrix $\gamma_{(+1)}^2$ coincides with γ^2 used in the discussion above. The spinor fields realizing the inequivalent representations we will denote by $\psi_{(s)}$. The corresponding Lagrangian densities read $L_s = \bar{\psi}_{(s)}(i\gamma_{(s)}^\mu D_\mu - m)\psi_{(s)}$. For massive fields the model with given s is not invariant under the parity and time-reversal transformations. In the absence of magnetic field we can construct fermionic models invariant under those transformations combining the

separate field in the Lagrangian density $L = \sum_{s=\pm 1} L_s$. The corresponding problem can be mapped to the problem we have considered in the previous text. In order to realize that let us introduce new fields $\psi'_{(s)}$ in accordance with $\psi'_{(s)} = \gamma^0 \gamma^{(1-s)/2} \psi_{(s)}$. In terms of those fields the Lagrangian density is rewritten as $L = \sum_{s=\pm 1} \bar{\psi}'_{(s)} (i\gamma^\mu D_\mu - sm) \psi'_{(s)}$, with the same set of gamma matrices as in (2.2).

Let assume that the fields $\psi_{(s)}$ in the initial representation obey the boundary conditions

$$(1 + \eta_{(s)} i n_\mu \gamma^\mu_{(s)}) \psi_{(s)} = 0, \quad r = a, \quad (7.1)$$

with $\eta_{(s)} = \pm 1$. The parameter $\eta_{(s)}$ may differ for the fields $s = +1$ and $s = -1$. In terms of new fields $\psi'_{(s)}$, the boundary conditions are transformed to

$$(1 + s \eta_{(s)} i n_\mu \gamma^\mu) \psi'_{(s)} = 0, \quad r = a. \quad (7.2)$$

Introducing the current densities for the fields $\psi_{(s)}$ and $\psi'_{(s)}$ by the standard formulas $j_{(s)}^\nu = e \bar{\psi}_{(s)} \gamma^\nu_{(s)} \psi_{(s)}$ and $j'_{(s)}^\nu = e \bar{\psi}'_{(s)} \gamma^\nu_{(s)} \psi'_{(s)}$, we obtain the following relations for the expectation values of the charge and current densities:

$$\langle j_{(s)}^\nu \rangle = s^{\nu/2} \langle j'_{(s)}^\nu \rangle, \quad (7.3)$$

for $\nu = 0, 2$. The fields $\psi'_{(s)}$ obey the equation (2.2) and the boundary conditions (7.2).

From the discussion at the end of Section 5 it follows that the expressions for the expectation values $\langle j'_{(s)}^\nu \rangle$ are related to the charge and current densities presented in the previous sections by the formula

$$\langle j'_{(s)}^\nu \rangle = (s \eta_{(s)})^{1-\nu/2} \langle j^\nu \rangle_{(\eta_{(s)}, s \eta_{(s)} \mu, +1)}. \quad (7.4)$$

By using the relation (7.3), the charge ($\nu = 0$) and current ($\nu = 2$) densities for the initial fields $\psi_{(s)}$ are expressed as

$$\langle j_{(s)}^\nu \rangle = s \eta_{(s)}^{1-\nu/2} \langle j^\nu \rangle_{(\eta_{(s)}, s \eta_{(s)} \mu, +1)}. \quad (7.5)$$

For the total expectation values in models with Lagrangian density $L = \sum_{s=\pm 1} L_s$ one gets

$$\langle J^\nu \rangle = \sum_{s=\pm 1} s \eta_{(s)}^{1-\nu/2} \langle j^\nu \rangle_{(\eta_{(s)}, s \eta_{(s)} \mu, +1)}. \quad (7.6)$$

From here it follows that if the fields $\psi_{(s)}$ obey the same boundary condition ($\eta_{(+1)} = \eta_{(-1)}$) then

$$\langle J^\nu \rangle = \eta_{(+1)}^{1-\nu/2} \sum_{s=\pm 1} s \langle j^\nu \rangle_{(\eta_{(+1)}, s \eta_{(+1)} \mu, +1)}, \quad (7.7)$$

and the total charge and current densities are zero for $\mu = 0$. In this special case, the expectation values are odd functions of the chemical potential. Now, by taking into account that $\langle j^\nu \rangle(-\alpha_0, -\mu) = -\langle j^\nu \rangle(\alpha_0, \mu)$, we conclude that the expectation value $\langle J^\nu \rangle$ is an odd function of α_0 . For the fields $\psi_{(s)}$ obeying different boundary conditions ($\eta_{(+1)} = -\eta_{(-1)}$, the fields $\psi'_{(s)}$ obey the same boundary conditions), the formula (7.6) is reduced to

$$\langle J^\nu \rangle = \eta_{(+1)}^{1-\nu/2} \left[\langle j^\nu \rangle_{(\eta_{(+1)}, \eta_{(+1)} \mu, +1)} - (-1)^{1-\nu/2} \langle j^\nu \rangle_{(-\eta_{(+1)}, \eta_{(+1)} \mu, +1)} \right]. \quad (7.8)$$

For a massless field one has $\langle j^\nu \rangle_{(-\eta_{(+1)}, \eta_{(+1)} \mu, +1)} = \langle j^\nu \rangle_{(\eta_{(+1)}, \eta_{(+1)} \mu, +1)}$ and the total current density in (7.8) vanishes, $\langle J^2 \rangle = 0$. For the charge density one gets $\langle J^0 \rangle = 2\eta_{(+1)} \langle j^0 \rangle_{(\eta_{(+1)}, \eta_{(+1)} \mu, +1)}$. Note that, in general, the fields $\psi_{(+1)}$ and $\psi_{(-1)}$ may have different masses and in the corresponding problems there will be no cancellations between the separate contributions of those field into the total expectation values.

The spinor fields $\psi_{(s)}$ appear in the Dirac model describing the long wavelength properties of the electronic subsystem of graphene. The parameter s enumerates the valley degrees of freedom and

corresponds to the points \mathbf{K}_+ and \mathbf{K}_- of the graphene Brillouin zone. The spinors are presented as $\psi_{(s)} = (\psi_{s,AS}, \psi_{s,BS})^T$, where the upper and lower components are expressed in terms of the electron wave functions on the A and B sites of the graphene lattice and $S = +1$ and $S = -1$ correspond to additional degree of freedom related to spin. The Dirac equation describing the dynamics of the subsystem of π -electrons can be expressed in terms of four-component spinors $\Psi_S = (\psi_{(+1)}, \psi_{(-1)})^T$ introducing the 4×4 Dirac matrices $\gamma_{(4)}^\mu = \sigma_{P3} \otimes \gamma^\mu$ and the related spin connection $\Gamma_\mu^{(4)} = I \otimes \Gamma_\mu$ with $\sigma_{P3} = \text{diag}(1, -1)$ and $I = \text{diag}(1, 1)$. In the part containing the spatial derivatives, the speed of light is replaced by the Fermi velocity of electrons $v_F \approx 7.9 \times 10^7 \text{ cm/s}$. The mass m in the corresponding Dirac equation is expressed in terms of the energy gap Δ by the relation $m = \Delta/v_F^2$ and for the corresponding Compton wavelength one has (in standard units) $\lambda_C = \hbar v_F/\Delta$. Several mechanisms have been considered in the literature for the generation of the gap in the range $1 \text{ meV} \lesssim \Delta \lesssim 1 \text{ eV}$. In translating the results given above for graphene nanocones the replacement $m \rightarrow 1/\lambda_C$ should be done and an additional factor v_F appears in the definition of the spatial components of the current density operator. In graphene nanocones the possible values of the planar angle deficit are dictated by the symmetry of the hexagonal lattice and are given by $2\pi - \phi_0 = \pi n_c/3$ with $n_c = 1, 2, \dots, 5$ (for effects of conical topology on the electronic properties of graphene see, e.g., [17]-[25] and references therein). The graphitic cones with these values of opening angle have been experimentally observed [16].

8 Conclusion

We have investigated the impact of a circular edge of a 2D conical space on the expectation values of the charge and current densities for a massive spinor field in thermal equilibrium at temperature T . In the presence of an external gauge field the Dirac equation is presented as (2.2), where the parameter s in front of the mass term describes the two inequivalent irreducible representations of the Clifford algebra. For conical geometry, the general case of the planar angle deficit is considered. The edge at the radial coordinate $r = a$ divides the space into two causally separated regions: I- and E-regions for $r < a$ and $r > a$, respectively. On the edge the field operator is constrained by the boundary condition (2.8). In the I-region that leads to the discretization of the radial quantum number γ with the eigenvalues being the roots of the equation (2.17). In the E-region the spectrum of γ is continuous. The complete set of spinor modes is given by (2.10) with the radial functions expressed as (2.13) in the I- and E-regions. The expectation values of the charge and current densities are decomposed into three parts corresponding to the VEVs and contributions coming from particles and antiparticles (see (2.24)). They are presented in the form of sums over the spinorial modes. We have explicitly separated from those mode sums the edge induced contributions. In the I-region that is done by the application of the Abel-Plana type summation formula (5.8) to the series over the eigenvalues of the radial quantum number. In the corresponding integral representation of the edge-induced expectation values the explicit knowledge of those eigenvalues is not required. Note that the current density considered above is the analog of the persistent currents in normal metal rings predicted in [56] and experimentally confirmed in a number of papers (see, e.g., [57, 58]). That type of currents may appear also in a number of other mesoscopic condensed matter system such as graphene and topological insulator rings (see, for example, [59, 60, 61, 62, 63] and references given in [44, 64]).

The mean radial current density vanishes and the finite temperature boundary-induced contributions in the expectation values of the charge and azimuthal current densities are given by the expressions (4.10) in the E-region and by (5.15) in the I-region, with u_n from (4.9). The influence of the magnetic flux on the expectation values is of Aharonov-Bohm type effect and, as expected, they are periodic with respect to the magnetic flux with the period of flux quantum. In addition, the charge and current densities are odd functions under the reflection $(\alpha_0, \mu) \rightarrow (-\alpha_0, -\mu)$ in the space of the parameter α_0 , determining the fractional part of the magnetic flux (in units of flux quantum), and the chemical potential. In particular, for $\alpha_0 = 0$ the VEVs vanish and the net charge and current densities for the nonzero

chemical potential are purely finite temperature effect. For the special case of zero chemical potential the arguments of the modified Bessel functions in general formulas are real and the corresponding expressions are reduced to (4.14) and (5.18) in the E- and I-regions, respectively. For a massless field the further simplifications lead to the representations (4.15) and (5.19). An important difference from the fermionic condensate, considered in [45] (see also [65] for the corresponding problem in the case of two circular boundaries at zero temperature), is that the charge and current densities are finite on the boundary. The corresponding thermal contributions are connected by the relations (4.4) and (5.3) for the E- and I-regions, respectively. Having the expectation values for the boundary condition (2.8) one can obtain the corresponding expressions for the charge and current densities in the case of the condition that differs from (2.8) by the sign of the term containing the normal vector (the boundary condition (5.22) with $\eta = -1$). The expectation values in problems with two sets of parameters (s, μ, η) and $(-s, -\mu, -\eta)$ are connected by the relation (5.24). Another extension of the obtained results corresponds to fields with more general periodicity condition with respect to the angular coordinate ϕ . As it has been shown at the end of Section 5, the nontrivial phase in the respective quasiperiodicity condition can be interpreted in terms of the effective magnetic flux and vice versa.

General formulas for the expectation values are rather complicated. To clarify the behavior of the charge and current densities we have considered different asymptotic regions of the parameters. In the E-region, at large distances from the boundary and for a massive field the expectation value of the charge density is dominated by the Minkowskian part $\langle j^0 \rangle_M^{(0)}$ which does not depend on r . Contrary to that, the expectation value of the current density decays exponentially at large distances. In the I-region and for small values of the radial coordinate r the boundary-induced current density tends to zero, whereas the boundary-induced charge density tends to zero for $2|\alpha_0| < 1 - 1/q$ and diverges in the range $2|\alpha_0| > 1 - 1/q$. In the last case, near the cone apex, for a massive field the expectation values of the charge and current densities in the boundary-free geometry are dominated by the vacuum parts. If the radial coordinate is held constant and the circular boundary is brought closer to the apex, then in the limit of small values of a , the boundary-induced expectation values in the E-region will tend to zero for $|\alpha_0| < 1/2$.

The expectation values at half-integer values of the ratio of magnetic flux to flux quantum (corresponding to half-integer values of the parameter α) are obtained from the general formulas in the limit $\alpha_0 \rightarrow \pm 1/2$. The limiting values in the boundary-free geometry are given by (6.13) and the corresponding charge and current densities are discontinuous at half-integer values of α . Similar discontinuities are present also in the boundary-induced parts and for $\alpha_0 = \pm 1/2$ they come from the contribution of the fermionic mode with $j = \mp 1/2$. They are given by the formulas (6.17) and (6.21) in the E- and I-regions, respectively. We have shown that in the E-region the discontinuities in the parts $\langle j^\nu \rangle^{(0)}$ and $\langle j^\nu \rangle^{(b)}$ are canceled out in the total expectation value $\langle j^\nu \rangle = \langle j^\nu \rangle^{(0)} + \langle j^\nu \rangle^{(b)}$ and the latter is continuous at half-integer values of α . This is related to the fact that all the spinorial modes in the E-region are regular. For zero chemical potential the expectation values are odd functions of α_0 and from the expressions for discontinuities one can find the corresponding values at $\alpha_0 = \pm 1/2$ (see Eqs. (6.18) and (6.22)).

At high temperatures, the boundary-induced expectation values of the charge and current densities for a given r are suppressed by the factor $e^{-2\pi T(r-a)}$. In that limit and for nonzero chemical potential the total charge density is dominated by the Minkowskian part with the high temperature behavior $\langle j^0 \rangle_M^{(0)} \propto \mu T$. For the current density independent of a one has $\langle j_\phi \rangle^{(0)} \propto e^{-2\pi T r \sin(\phi_0/2)}$ for $\phi_0 < \pi$ and $\langle j_\phi \rangle^{(0)} \propto e^{-2\pi T r}$ in the region $\phi_0 > \pi$. The zero temperature limit of the expectation values depends on the relative values of the mass and chemical potential. In the range $|\mu| < m$ the expectation values tend to the corresponding VEVs in the limit $T \rightarrow 0$. For the values of the chemical potential in the range $|\mu| > m$ the contributions of particles/antiparticles survive in the zero temperature limit. Those contributions come from particles for $\mu > 0$ and antiparticles for $\mu < 0$. They are given by the expressions (4.18) and (5.20).

In Section 7 we have shown that the expectation values of the charge and current densities for fields

realizing the second inequivalent irreducible representation of the Clifford algebra are obtained from the formulas presented in the preceding sections. For fields with boundary conditions (7.1) the corresponding relation is given by (7.5). In fermionic models invariant under parity and time-reversal transformations (in the absence of magnetic fields), combining fields in two inequivalent representations, the total expectation values are expressed by (7.6). We have considered different combinations of boundary conditions for separate fields. In the long wavelength description of the electronic subsystem in graphene, based on the Dirac model, the parameter s corresponds to the valley degrees of freedom. At the end of Section 7 we have discussed applications in graphene nanocones described by the effective field-theoretical model.

Acknowledgments

The work was supported by the grants No. 21AG-1C047 and 24FP-3B021 of the Higher Education and Science Committee of the Ministry of Education, Science, Culture and Sport RA.

A Transformation of the expectation values in the E-region

In this appendix we present the details of the transformations for the thermal expectation values in the E-region. They will be presented separately for nonzero and zero chemical potentials.

A.1 Nonzero chemical potential

For the case of nonzero chemical potential, $\mu \neq 0$, the integrands in (4.7) have branch points $\gamma = \pm im$ and simple poles $\gamma = \gamma_n^{(\lambda)}$, $n = 0, \pm 1, \pm 2, \dots$, in the complex plane γ . The poles, given by (5.6), are located in the right half-plane for $\lambda\mu > 0$ and in the left half-plane for $\lambda\mu < 0$. Other features of the locations for the poles are described in Section 5.

By taking into account that for $r > a$ and $l = 1$ ($l = 2$) the integrands in (4.7) exponentially decrease in the upper (lower) half-plane for $|\gamma| \gg 1$, in the integrals over γ we rotate the contour by the angle $\pi/2$ ($-\pi/2$). The integrals over $\gamma \in [0, \infty)$ are transformed to the integrals over the imaginary axis of the complex plane γ (over $\gamma \in [0, i\infty)$ for $l = 1$ and $\gamma \in [0, -i\infty)$ for $l = 2$). For $\lambda\mu > 0$ the parts involving the residues at the poles $\gamma = \gamma_n^{(\lambda)}$ have to be added. Using the relation $\sqrt{(\pm i\gamma)^2 + m^2} = \sqrt{m^2 - \gamma^2}$ for $0 \leq \gamma \leq m$ and the definition (2.15), it can be seen that the integrals over the intervals $[0, im]$ and $[0, -im]$ cancel each other. Introducing the modified Bessel functions in the integrals over the intervals $[im, i\infty)$ and $[-im, -i\infty)$, and also in the residue terms, we obtain the representation

$$\begin{aligned} \langle j^0 \rangle_{T\lambda}^{(b)} = & \frac{e}{\pi\phi_0} \sum_j \sum_{\chi=\pm 1} \left\{ - \int_m^\infty dx x \operatorname{Re} \left[\frac{\tilde{I}_{\beta_j}^{(\lambda)}(xa)}{\tilde{K}_{\beta_j}^{(\lambda)}(xa)} \frac{K_{\alpha_j-\chi\epsilon_j/2}^2(xr)}{e^{\beta(i\sqrt{x^2-m^2}-\lambda\mu)} + 1} \frac{sm + \lambda\chi i\sqrt{x^2-m^2}}{\sqrt{x^2-m^2}} \right] \right. \\ & \left. + 2\pi T \theta(\lambda\mu) \sum_{n=0}^\infty \operatorname{Re} \left[\frac{\tilde{I}_{\beta_j}^{(\lambda)}(u_n^{(\lambda)}a)}{\tilde{K}_{\beta_j}^{(\lambda)}(u_n^{(\lambda)}a)} [\chi\mu + sm + \lambda\chi i\pi(2n+1)T] K_{\alpha_j-\chi\epsilon_j/2}^2(u_n^{(\lambda)}r) \right] \right\}, \end{aligned} \quad (\text{A.1})$$

for the boundary-induced contribution in the thermal part of the charge density. Here, the notations (5.7) and (5.9) have been used. In the similar way, for the corresponding azimuthal current density one gets

$$\begin{aligned} \langle j^2 \rangle_{T\lambda}^{(b)} = & \frac{e}{\pi\phi_0} \sum_j \left\{ - \int_m^\infty dx \frac{x U_{2,\beta_j}^K(xr)}{\sqrt{x^2-m^2}} \operatorname{Re} \left[\frac{\tilde{I}_{\beta_j}^{(\lambda)}(xa)}{\tilde{K}_{\beta_j}^{(\lambda)}(xa)} \frac{1}{e^{\beta(i\sqrt{x^2-m^2}-\lambda\mu)} + 1} \right] \right. \\ & \left. + 2\pi T \theta(\lambda\mu) \sum_{n=0}^\infty \operatorname{Re} \left[\frac{\tilde{I}_{\beta_j}^{(\lambda)}(u_n^{(\lambda)}a)}{\tilde{K}_{\beta_j}^{(\lambda)}(u_n^{(\lambda)}a)} U_{2,\beta_j}^K(u_n^{(\lambda)}r) \right] \right\}. \end{aligned} \quad (\text{A.2})$$

Note that $\gamma_n^{(\lambda)} = iu_n^{(\lambda)}$ and $u_n^{(-)} = u_n^{(+)*}$. By taking into account the relations (5.11), the expressions (A.1) and (A.2) are transformed to (4.8).

A.2 Zero chemical potential

In the case of zero chemical potential, $\mu = 0$, for the poles of the integrands in (4.7) located in the upper half-plane of complex variable γ we have $\gamma = \gamma_n = iu_{0n}$, $n = 0, 1, 2, \dots$, with u_{0n} defined in (4.13). The poles in the lower half-plane are expressed as $\gamma_n = \gamma_{-n-1}^*$ with $n = \dots, -2, -1$. All the poles are located on the imaginary axis. Similar to the case $\mu \neq 0$, in the separate integrals of (4.7) with $l = 1, 2$ we rotate the contours by the angle $(-1)^{l-1}\pi/2$ bypassing the poles γ_n on the imaginary axis by semi-circular arcs $C_\rho(\gamma_n)$ of small radius ρ . These arcs pass around the poles clockwise in the upper half-plane and counter-clockwise in the lower half-plane. It can be seen that the sum of the integrals along $C_\rho(\gamma_n)$ with $n = \dots, -2, -1$ is the complex conjugate of the sum of the integrals with $n = 0, 1, 2, \dots$. In the limit $\rho \rightarrow 0$ the sum of the integrals over the straight segments gives the principal values of the integrals over the positive and negative imaginary semiaxes (denoted here as p.v.). The integrals over the intervals $[0, im]$ and $[0, -im]$ cancel each other, whereas the integral over $[-im, -i\infty)$ is the complex conjugate of the integral over $[im, i\infty)$. Introducing the modified Bessel functions, we get

$$\begin{aligned} \langle j^0 \rangle_{T\lambda}^{(b)} &= \frac{e}{\pi\phi_0} \sum_j \sum_{\chi=\pm 1} \left\{ -\text{p.v.} \int_m^\infty d\gamma \frac{\gamma K_{\alpha_j-\chi\epsilon_j/2}^2(\gamma r)}{\sqrt{\gamma^2 - m^2}} \text{Re} \left[\frac{\bar{I}_{\beta_j}^{(\lambda)}(\gamma a)}{\bar{K}_{\beta_j}^{(\lambda)}(\gamma a)} \frac{sm + \lambda\chi i\sqrt{\gamma^2 - m^2}}{e^{i\beta\sqrt{\gamma^2 - m^2}} + 1} \right] \right. \\ &\quad \left. + \pi T \sum_{n=0}^\infty \text{Re} \left[\frac{\bar{I}_{\beta_j}^{(\lambda)}(u_{0n}a)}{\bar{K}_{\beta_j}^{(\lambda)}(u_{0n}a)} [sm + \lambda\chi i\pi(2n+1)T] K_{\alpha_j-\chi\epsilon_j/2}^2(u_{0n}r) \right] \right], \\ \langle j^2 \rangle_{T\lambda}^{(b)} &= \frac{e}{\pi\phi_0} \sum_j \left\{ -\text{p.v.} \int_m^\infty d\gamma \frac{\gamma U_{2,\beta_j}^K(\gamma r)}{\sqrt{\gamma^2 - m^2}} \text{Re} \left[\frac{\bar{I}_{\beta_j}^{(\lambda)}(\gamma a)}{\bar{K}_{\beta_j}^{(\lambda)}(\gamma a)} \frac{1}{e^{i\beta\sqrt{\gamma^2 - m^2}} + 1} \right] \right. \\ &\quad \left. + \pi T \sum_{n=0}^\infty \text{Re} \left[\frac{\bar{I}_{\beta_j}^{(\lambda)}(u_{0n}a)}{\bar{K}_{\beta_j}^{(\lambda)}(u_{0n}a)} \right] U_{2,\beta_j}^K(u_{0n}r) \right\}. \end{aligned} \quad (\text{A.3})$$

Here, the parts involving the series over n come from the integrals along the contours $C_\rho(\gamma_n)$ and the parts with the integrals over γ are the contributions from the integrals over the straight segments on the imaginary axis. Now, we need to evaluate the thermal contribution in the boundary-induced expectation values as the sum $\langle j^\nu \rangle_T^{(b)} = \sum_{\lambda=\pm} \langle j^\nu \rangle_{T\lambda}^{(b)}$. By using the relations $\bar{F}_{\beta_j}^{(-)}(z) = \bar{F}_{\beta_j}^{(+)*}(z)$, $F = I, K$, we can see that the contributions coming from the first terms in the right-hand side for each expectation value in (A.3) to the sum over λ give $-\langle j^\nu \rangle_{\text{vac}}^{(b)}$ which are given by (3.7). In this way we find

$$\begin{aligned} \langle j^0 \rangle_T^{(b)} &= \frac{2eT}{\phi_0} \sum_j \sum_{n=0}^\infty \text{Re} \left[\frac{\bar{I}_{\beta_j}(u_{0n}a)}{\bar{K}_{\beta_j}(u_{0n}a)} \sum_{\chi=\pm 1} [sm + \chi i\pi(2n+1)T] K_{\alpha_j-\chi\epsilon_j/2}^2(u_{0n}r) \right] - \langle j^0 \rangle_{\text{vac}}^{(b)}, \\ \langle j^2 \rangle_T^{(b)} &= \frac{2eT}{\phi_0} \sum_j \sum_{n=0}^\infty \text{Re} \left[\frac{\bar{I}_{\beta_j}(u_{0n}a)}{\bar{K}_{\beta_j}(u_{0n}a)} \right] U_{2,\beta_j}^K(u_{0n}r) - \langle j^2 \rangle_{\text{vac}}^{(b)}. \end{aligned} \quad (\text{A.4})$$

Substituting (A.4) into (3.3), for the total boundary-induced expectation values $\langle j^\nu \rangle^{(b)}$ in the case of zero chemical potential we get (4.14). The corresponding formulae are also obtained from (4.10) in the limit $\mu \rightarrow 0$.

B Zero temperature limit

In the main text we have considered the zero temperature limit of the charge and current densities started from the initial representations (4.1) and (5.1). In this appendix we show that the same results are obtained started from (4.10) and (5.15). To be short, the presentation of the limiting transition will be given for the current density only. The corresponding steps for the charge density are similar. In the E-region and for small temperatures the series over n in (4.10) is dominated by the contribution of the terms with large n and we replace the corresponding summation by the integration in accordance with $\sum_{n=0}^{\infty} f(u_n) \rightarrow \frac{1}{2\pi T} \int_{-i\mu}^{\infty-i\mu} dx f(u)$, where $u = (x^2 + m^2)^{1/2}$. The leading order term, obtained in this way, does not depend on the temperature and one gets

$$\lim_{T \rightarrow 0} \langle j^2 \rangle^{(b)} = \frac{e}{\pi \phi_0} \sum_j \operatorname{Re} \left[\int_{-i\mu}^{\infty-i\mu} dx \frac{\bar{I}_{\beta_j}(ua)}{\bar{K}_{\beta_j}(ua)} U_{2,\beta_j}^K(ur) \right]. \quad (\text{B.1})$$

By taking into account that for $r > a$ the integrand is exponentially small for large values of $a \operatorname{Re} u$, the integral in (B.1) is transformed to the sum of the integrals over the straight contours $[-i\mu, 0]$ and $[0, \infty)$. Comparing with (3.7), we see that the part coming from the integral over $[0, \infty)$ coincides with the boundary-induced vacuum current density $\langle j^2 \rangle_{\text{vac}}^{(b)}$. The remaining part with the integral over $[-i\mu, 0]$ is the contribution from particles and antiparticles. In the case $|\mu| < m$ we pass to the integral over $y = -ix$ with $\int_{-i\mu}^0 dx = i \int_{-\mu}^0 dy$. In the new integral one has $u = \sqrt{m^2 - y^2}$ and $0 < u < m$. In this range, all the functions in the integrand of (B.1) are real and the real part of integral $i \int_{-\mu}^0 dy$ is zero. Hence, for $|\mu| < m$ we get $\lim_{T \rightarrow 0} \langle j^2 \rangle^{(b)} = \langle j^2 \rangle_{\text{vac}}^{(b)}$, in agreement with (4.17).

In the range $|\mu| > m$ for the chemical potential the integral over $[-i\mu, 0]$ is further decomposed into the sum of the integrals over $[-i\mu, -\lambda im]$ and $[-\lambda im, 0]$, with $\lambda = \pm$ defined in accordance with $\mu = \lambda|\mu|$. By the arguments similar to those used for the integral over $[-i\mu, 0]$ in the case $|\mu| < m$, we can see that the real part of the integral over $[-\lambda im, 0]$ is zero. In the remaining integral over the region $[-i\mu, -\lambda im]$ we introduce $y = e^{\lambda i\pi/2} x$ and then pass to the integration over $\gamma = \sqrt{y^2 - m^2}$. As a result, the integral is transformed as

$$\int_{-\lambda i|\mu|}^{-\lambda im} dx f(u) = \lambda i \int_0^{\gamma_F} d\gamma \frac{\gamma}{E} f(e^{-\lambda i\pi/2} \gamma), \quad (\text{B.2})$$

where $f(u)$ is the integrand in (B.1) and, as before, $E = \sqrt{\gamma^2 + m^2}$. Next, in the right-hand side of (B.2) we return to the Bessel and Hankel functions by using the relations

$$\bar{I}_{\beta_j}(e^{-\lambda i\pi/2} u) = e^{-\lambda i\pi\beta_j/2} \bar{J}_{\beta_j}^{(\lambda)}(u), \quad \bar{K}_{\beta_j}(e^{-\lambda i\pi/2} u) = \frac{\lambda\pi i}{2} e^{\lambda i\pi\beta_j/2} \bar{H}_{\beta_j}^{(l,\lambda)}(u), \quad (\text{B.3})$$

where $l = 1$ ($l = 2$) for $\lambda = +$ ($\lambda = -$) and the notation $\bar{F}_{\beta_j}^{(\pm)}(z)$ for the Bessel and Hankel functions is defined by (2.15). Finally, the edge induced contribution in the E-region is expressed as

$$\lim_{T \rightarrow 0} \langle j^2 \rangle^{(b)} = \langle j^2 \rangle_{\text{vac}}^{(b)} - \frac{e}{\phi_0 r} \sum_j \epsilon_j \int_0^{\gamma_F} d\gamma \frac{\gamma^2}{E} \operatorname{Re} \left[\frac{\bar{J}_{\beta_j}^{(\lambda)}(\gamma a)}{\bar{H}_{\beta_j}^{(l,\lambda)}(\gamma a)} H_{\beta_j}^{(l)}(\gamma r) H_{\beta_j + \epsilon_j}^{(l)}(\gamma r) \right]. \quad (\text{B.4})$$

Note that in the integration range of (B.4) the function $\bar{J}_{\beta_j}^{(\lambda)}(za)$ is real and the real part in the integrand is the same for $l = 1$ and $l = 2$. Adding to (B.4) the corresponding limit for the contribution independent of a , expressed as (4.19), and by using the identity (4.6), we obtain the result (4.18), as was expected.

Now we turn to the zero temperature limit of the current density in the I-region based on the representation (5.15) for the boundary-induced contribution. The leading order term in the corresponding asymptotic expansion is obtained replacing the summation over n by the integration. That term does not

depend on the temperature and gives the zero temperature limit. Similar to (B.1), the current density it is presented in the form

$$\lim_{T \rightarrow 0} \langle j^2 \rangle^{(b)} = \frac{e}{\pi \phi_0} \sum_j \operatorname{Re} \left[\int_{-i\mu}^{\infty-i\mu} dx \frac{\bar{K}_{\beta_j}(ua)}{\bar{I}_{\beta_j}(ua)} U_{2,\beta_j}^I(ur) \right], \quad (\text{B.5})$$

again, with $u = (x^2 + m^2)^{1/2}$. Now we deform the integration contour in the way described above for the E-region. The part of the integral over $x \in [0, \infty)$ gives the VEV $\langle j^2 \rangle_{\text{vac}}^{(b)}$ (see (3.7)). For $|\mu| < m$, we introduce in the integral $\int_{-i\mu}^0 dx$ new variable $y = -ix$ with $u = \sqrt{m^2 - y^2} > 0$. In this case the functions in the integrand of (B.5) are real and for the part of the integral $\int_{-i\mu}^0 dx = i \int_{-\mu}^0 dy$ the real part is zero. The same arguments are valid in the case $|\mu| > m$ for the part of the integral $\int_{-i\mu}^0 dx$ over the interval $[-\lambda i m, 0]$. By transformations similar to those for (B.2) we can pass from the integral $\int_{-\lambda i |\mu|}^{-\lambda i m} dx$ to the integral $\int_0^{\gamma_F} d\gamma$. Passing to the Bessel and Hankel functions by using the relations (B.3), the function in the integrand is transformed as

$$\int_{-\lambda i |\mu|}^{-\lambda i m} dx \frac{\bar{K}_{\beta_j}(ua)}{\bar{I}_{\beta_j}(ua)} U_{2,\beta_j}^I(ur) = -\lambda \frac{\pi}{2} \int_0^{\gamma_F} d\gamma \frac{\bar{H}_{\beta_j}^{(l,\lambda)}(\gamma a)}{\bar{J}_{\beta_j}^{(\lambda)}(\gamma a)} g^{(2)}(\gamma), \quad (\text{B.6})$$

where $u = e^{-\lambda \pi i/2} \gamma$, the function $g^{(2)}(\gamma)$ is defined by (5.2), and l is the same as in (B.3). An important difference from the E-region is that now the integrand in (B.6) has poles $\gamma = \gamma_{j,l}^{(\lambda)}/a$, $l = 1, \dots, l_m$, with l_m defined in accordance with (5.21). These poles have to be avoided by semicircles $C_\rho(\gamma_{j,l}^{(\lambda)})$, with small radius ρ , in the right half-plane. The integral in the right-hand side of (B.6) should be understood as

$$\int_0^{\gamma_F} d\gamma = \text{p.v.} \int_0^{\gamma_F} d\gamma + \lim_{\rho \rightarrow 0} \sum_{l=1}^{l_m}' \int_{C_\rho(\gamma_{j,l}^{(\lambda)})} d\gamma. \quad (\text{B.7})$$

Here the prime means that in case $\gamma_{j,l_m}^{(\lambda)} = a\gamma_F$ the integral $\int_{C_\rho(\gamma_{j,l_m}^{(\lambda)})} d\gamma$ is taken over the quarter circle $C_\rho(\gamma_{j,l_m}^{(\lambda)})$ with its center located at $\gamma = \gamma_F$. The real part of the first integral in the right-hand side of (B.7) gives $\int_0^{\gamma_F} d\gamma g^{(2)}(\gamma)$ and the corresponding contribution to (B.5) is expressed as $\langle j^2 \rangle_{\text{vac}}^{(0)} - \langle j^2 \rangle_{T=0}^{(0)}$. The contours $C_\rho(\gamma_{j,l}^{(\lambda)})$ in (B.7) are determined by the condition that the poles $x = -\lambda i \sqrt{\gamma_{j,l}^{(\lambda)2}/a^2 + m^2}$ in the left-hand side of (B.6) are avoided by small semicircles in the right half-plane of complex variable x . From that condition it follows that in (B.7) $C_\rho(\gamma_{j,l}^{(\lambda)})$ is a semicircular contour in the upper/lower half-plane of complex variable γ , centered at $\gamma = \gamma_{j,l}^{(\lambda)}$, with clockwise/counter-clockwise directions for $\lambda = +/\lambda = -$. The corresponding integral is expressed in terms of the respective residue: $\int_{C_\rho(\gamma_{j,l}^{(\lambda)})} d\gamma = -\lambda \pi i \operatorname{Res}_{\gamma=\gamma_{j,l}^{(\lambda)}/a}$. In the evaluation of the residue with the integrand from the right-hand side of (B.6) we use the relations

$$\bar{J}_{\beta_j}^{(\lambda)'}(z) = \frac{-2}{T_{\beta_j}^{(\lambda)}(z) J_{\beta_j}(z)}, \quad \bar{Y}_{\beta_j}(z) = \frac{2}{\pi J_{\beta_j}(z)}, \quad (\text{B.8})$$

for $z = \gamma_{j,l}^{(\lambda)}$. Collecting all the contributions to the right-hand side of (B.5) we get

$$\lim_{T \rightarrow 0} \langle j^2 \rangle^{(b)} = \langle j^2 \rangle_{\text{vac}} - \langle j^2 \rangle_{T=0}^{(0)} + \frac{\lambda e}{2\phi_0 a} \sum_j \sum_{l=1}^{l_m}' T_{\beta_j}^{(\lambda)}(a\gamma_{j,l}^{(\lambda)}) g^{(2)}(\gamma_{j,l}^{(\lambda)}), \quad (\text{B.9})$$

which is equivalent to (5.20).

References

- [1] E. Fradkin, *Field Theory of Condensed Matter Systems* (Cambridge University Press, Cambridge, 2013).
- [2] N. Nagaosa, *Quantum Field Theory in Condensed Matter Physics and Quantum Field Theory in Strongly Correlated Electronic Systems* (Springer, Berlin, 1999).
- [3] R. Jackiw, Nucl. Phys. B **252**, 343 (1985).
- [4] V.P. Gusynin, S.G. Sharapov, and J.P. Carbotte, Int. J. Mod. Phys. B **21**, 4611 (2007).
- [5] A.H. Castro Neto, F. Guinea, N.M.R. Peres, K.S. Novoselov, and A.K. Geim, Rev. Mod. Phys. **81**, 109 (2009).
- [6] X.-L. Qi and S.-C. Zhang, Rev. Mod. Phys. **83**, 1057 (2011).
- [7] A. Muñoz de las Heras, E. Macaluso, and I. Carusotto, Phys. Rev. X **10**, 041058 (2020).
- [8] V.M. Mostepanenko and N.N. Trunov, *The Casimir Effect and Its Applications* (Clarendon, Oxford, 1997).
- [9] K.A. Milton, *The Casimir Effect: Physical Manifestation of Zero-Point Energy* (World Scientific, Singapore, 2002).
- [10] M. Bordag, G.L. Klimchitskaya, U. Mohideen, and V.M. Mostepanenko, *Advances in the Casimir Effect* (Oxford University Press, New York, 2009).
- [11] *Casimir Physics*, edited by D. Dalvit, P. Milonni, D. Roberts, and F. da Rosa, Lecture Notes in Physics Vol. 834 (Springer-Verlag, Berlin, 2011).
- [12] S. Bellucci, J. González, P. Onorato, and E. Perfetto, Phys. Rev. B **74**, 045427 (2006).
- [13] T.W. Kibble, J. Phys. A **9**, 1387 (1976).
- [14] A. Vilenkin and E.P.S. Shellard, *Cosmic Strings and Other Topological Defects* (Cambridge University Press, Cambridge, England, 1994).
- [15] M. Ge and K. Sattler, Chem. Phys. Lett. **220**, 192 (1994).
- [16] A. Krishnan, et al, Nature **388**, 451 (1997).
- [17] P.E. Lammert and V.H. Crespi, Phys. Rev. Lett. **85**, 5190 (2000).
- [18] J.-Ch. Charlier and G.-M. Rignanese, Phys. Rev. Lett. **86**, 5970 (2001).
- [19] V.A. Osipov and E.A. Kochetov, JETP Letters **73**, 562 (2001).
- [20] P.E. Lammert and V.H. Crespi, Phys. Rev. B **69**, 035406 (2004).
- [21] A. Cortijo and M.A.H. Vozmediano, Nucl. Phys. B **763**, 293 (2007).
- [22] C. Furtado, F. Moraes, and A.M.M. Carvalho, Phys. Lett. A **372**, 5368 (2008).
- [23] S.N. Naess, A. Elgsaeter, G. Helgesen, and K.D. Knudsen, Sci. Technol. Adv. Mater. **10**, 065002 (2009).
- [24] P. Ulloa, A. Latgé, L. E. Oliveira, and M. Pacheco, Nanoscale Research Letters **8**, 384 (2013).

[25] S. H. Mattoso, V. Brumas, S. Evangelisti, G. Fronzoni, T. Leininger, M. Stener, *J. Phys. Chem. A* **127**, 9723 (2023).

[26] S. Bellucci, I. Brevik, A. A. Saharian, and H. G. Sargsyan, *Eur. Phys. J. C* **80**, 281 (2020).

[27] L. Sriramkumar, *Classical Quantum Gravity* **18**, 1015 (2001).

[28] Yu.A. Sitenko and N.D. Vlasii, *J. Phys. A: Math. Theor.* **41**, 164034 (2008).

[29] Yu.A. Sitenko and N.D. Vlasii, *Classical Quantum Gravity* **26**, 195009 (2009).

[30] E.R. Bezerra de Mello, *Classical Quantum Gravity* **27**, 095017 (2010).

[31] E.R. Bezerra de Mello, V. Bezerra, A.A. Saharian, and V.M. Bardeghyan, *Phys. Rev. D* **82**, 085033 (2010).

[32] A. Mohammadi, E.R. Bezerra de Mello, and A.A. Saharian, *J. Phys. A: Math. Theor.* **48**, 185401 (2015).

[33] E.A.F. Bragança, H.F. Santana Mota, and E.R. Bezerra de Mello, *Int. J. Mod. Phys. D* **24**, 1550055 (2015).

[34] S. Bellucci, E.R. Bezerra de Mello, E. Bragança, and A.A. Saharian, *Eur. Phys. J. C* **76**, 359 (2016).

[35] A. Mohammadi and E.R. Bezerra de Mello, *Phys. Rev. D* **93**, 123521 (2016).

[36] Yu.A. Sitenko and N.D. Vlasii, *Universe* **4**, 23 (2018).

[37] A.A. Saharian, *Phys. Rev. D* **110**, 065020 (2024).

[38] E.R. Bezerra de Mello, V.B. Bezerra, A.A. Saharian, and H.H. Harutyunyan, *Phys. Rev. D* **91**, 064034 (2015).

[39] W. Oliveira dos Santos, H.F. Santana Mota, and E.R. Bezerra de Mello, *Phys. Rev. D* **99**, 045005 (2019).

[40] E.A.F. Bragança, E.R. Bezerra de Mello, and A.Mohammadi, *Int. J. Mod. Phys. D* **29**, 2050103 (2020).

[41] S. Bellucci, W. Oliveira Dos Santos, and E.R. Bezerra de Mello, *Eur. Phys. J. C* **80**, 963 (2020).

[42] E.R. Bezerra de Mello, W. Oliveira dos Santos, and A.A. Saharian, *Phys. Rev. D* **106**, 125009 (2022).

[43] W. Oliveira dos Santos, H.F. Santana Mota, and E.R. Bezerra de Mello, arXiv:2409.05691.

[44] A.A. Saharian, *Symmetry* **16**, 92 (2024).

[45] A.A. Saharian, E.R. Bezerra de Mello and A.A. Saharyan, *Phys. Rev. D* **100**, 105014 (2019).

[46] C.G. Beneventano and E.M. Santangelo, *Int. J. Mod. Phys.: Conf. Series* **14**, 240 (2012).

[47] S. Bellucci, A.A. Saharian, and A.Kh. Grigoryan, *Phys. Rev. D* **94**, 105007 (2016).

[48] A.P. Prudnikov, Yu.A. Brychkov, and O.I. Marichev, *Integrals and Series* (Gordon and Breach, New York, 1986), Vol. 2.

[49] A.A. Saharian, *Izv. Akad. Nauk. Arm. SSR. Mat.* **22**, 166 (1987) [English translation: A. A. Saaryan, *Sov. J. Contemp. Math. Anal.* **22**, 70 (1987)].

[50] A.A. Saharian, *The Generalized Abel-Plana Formula with Applications to Bessel Functions and Casimir Effect* (Yerevan State University Publishing House, Yerevan, 2008) (arXiv:0708.1187).

[51] M.V. Berry and R.J. Mondragon, Proc. R. Soc. A **412**, 53 (1987).

[52] D. Deutsch and P. Candelas, Phys. Rev. D **20**, 3063 (1979).

[53] G. Kennedy, R. Critchley, and J.S. Dowker, Ann. Phys. **125**, 346 (1980).

[54] S. Bellucci and A.A. Saharian, Phys. Rev. D **79**, 085019 (2009).

[55] S. Bellucci, A.A. Saharian, and V.M. Bardeghyan, Phys. Rev. D **82**, 065011 (2010).

[56] M. Büttiker, Y. Imry, R. Landauer, Phys. Lett. A **96**, 365 (1983).

[57] H. Bluhm et al., Phys. Rev. Lett. **102**, 136802 (2009).

[58] A.C. Bleszynski-Jayich et al., Science **326**, 272 (2009).

[59] M.F. Lin and D.S. Chuu, Phys. Rev. B **57**, 6731 (1998).

[60] S. Latil, S. Roche, and A. Rubio, Phys. Rev. B **67**, 165420 (2003).

[61] P. Recher, B. Trauzettel, A. Rycerz, Y. Blanter, C. Beenakker, and A. Morpurgo, Phys. Rev. B **76**, 235404 (2007).

[62] Z. Wu, Z. Zhang, K. Chang, and F.M. Peeters, Nanotechnology **21**, 185201 (2010).

[63] P. Michetti and P. Recher, Phys. Rev. B **83**, 125420 (2011).

[64] F.R.V. Araújo, D.R. da Costa, A.J.C. Chaves, F.E. B. de Sousa, and J.M. Pereira Jr., J. Phys.: Condens. Matter **34**, 125503 (2022).

[65] A. Saharian, T. Petrosyan, and A. Hovhannisyan, Universe **7**, 73 (2021).